

9-1-1993

# Optimal Trajectory Planning for Spray Coating

John K. Antonio

*Optimal Trajectory Planning for Spray Coating*

Follow this and additional works at: <http://docs.lib.purdue.edu/ecetr>

---

Antonio, John K., "Optimal Trajectory Planning for Spray Coating" (1993). *ECE Technical Reports*. Paper 238.  
<http://docs.lib.purdue.edu/ecetr/238>

This document has been made available through Purdue e-Pubs, a service of the Purdue University Libraries. Please contact [epubs@purdue.edu](mailto:epubs@purdue.edu) for additional information.

# OPTIMAL TRAJECTORY PLANNING FOR SPRAY COATING

JOHN K. ANTONIO

TR-EE 93-29  
SEPTEMBER 1993



SCHOOL OF ELECTRICAL ENGINEERING  
PURDUE UNIVERSITY  
WEST LAFAYETTE, INDIANA 47907-1285

---

# Optimal Trajectory **Planning** for Spray **Coating**\*

*John K. Antonio*  
**jantonio@ecn.purdue.edu**  
(317) 494-6416

School of Electrical Engineering  
Purdue University  
1285 Electrical Engineering Building  
West Lafayette, IN 47907-1285

September 1993

\*This work was supported by the National Science Foundation under grant 8803017-ECD to the Engineering Research Center for Intelligent Manufacturing Systems.

## ABSTRACT

The problem of how to optimally traverse a spray applicator around a surface to be coated is formulated as a type of optimization problem known as a constrained variational problem. An optimal trajectory for a spray applicator is defined to be one that results in minimal variation in accumulated film thickness on the surface. The trajectory for an applicator is characterized by a six-dimensional vector function that specifies the position and orientation of the applicator at each instant of time. The surface to be coated is represented with a function. For each surface point and for each feasible position and orientation of the applicator, a value for the instantaneous rate of film accumulation is assumed to be known. Empirical data and/or estimates for these values can be readily incorporated in the formulation. By making realistic approximations, the proposed constrained variational problem is transformed into a finite dimensional constrained optimization problem. Numerical studies are included that illustrate the utility of the problem formulation and the effectiveness of applying standard nonlinear programming techniques for determining solutions.

## I. INTRODUCTION

### A. *Background*

High quality paint finish is an important factor in the sales of many manufactured products. The perceived quality of products such as automobiles, appliances, and furniture, can be strongly influenced by the quality of their painted surfaces. Spray applicators are commonly used in industry to apply paint to the surfaces of manufactured products. The task of consistently achieving high quality finishes from spray applicator systems is complicated by the sensitivity of the coating process relative to environmental conditions (e.g., ambient temperature, barometric pressure, and relative humidity) and parameters associated with the spray system itself (e.g., position and orientation of the applicator, paint injection pressure, and paint viscosity).

In very general terms, the process of spray coating involves first the atomization and then the spraying of a coating material (e.g., paint) toward a surface to be coated. Paints typically contain some type of solvent. As the solvent evaporates, liquid paint becomes, more viscous; it eventually becomes solid when all solvent has evaporated. As atomized droplets of paint are transported through the air from the applicator to the surface, a relatively large fraction of solvent evaporates from the droplets, because the ratio of surface area to volume is relatively high for small droplets. Therefore, by the time droplets strike the surface, the viscosities of the droplets are substantially larger than they were immediately after atomization. This increase in viscosity helps to prevent the paint from running and/or sagging on the surface [1]. However, if too much solvent is lost during the transportation phase, then the droplets will be too “dry” when they impact the surface and thus may not flow together well to form a uniform film. If too much solvent is present in the surface film, then as the paint dries, an undesirable effect known as solvent popping may occur whereby excessive solvent and occluded air in the

film escape by erupting through the surface [1]. Thus, solvent concentrations and solvent types are important factors to consider to achieve high quality finishes.

The types of solvents used in industry for spray painting have been the topic of much environmental and political concern in recent years. Since the signing of the Clean Air Act of 1970, the Environmental Protection Agency (EPA) has issued numerous ambient air standards. Among the many factors of air quality regulated by the EPA over the past two decades is the air's concentration of hydrocarbons and photochemical oxidants, which are present in some industrial solvents [18].

The complex interactions among the many parameters in a spray painting system are not well understood. Even heavily automated spray painting processes, such as those found in the automotive industry, are typically designed and/or tuned based on "rules of thumb" [20]. It is common practice for such painting facilities to initially set some of the system parameters (such as shaping air pressure, injection pressure, solvent concentration, and applied electrostatic voltage) by spraying several dozen "test panels" under various values for these parameters. A jury of paint experts then convene to examine the painted test panels and vote to establish a rank ordering of the panels based on a weighted collection of quality attributes. The parameter settings associated with the panel with the highest overall ranking are then used as set points on the production line for that day (or shift). Because a human's ability to make consistent judgments regarding paint quality are strongly influenced by his/her mood, levels of fatigue, and other factors, some facilities incorporate the use of optical/image sensing devices and signal processing techniques to automate the process of judging test panels [2, 11].

The "excellence of appearance" for a painted surface is somewhat subjective and the desired features of a finish generally depend on the nature and/or intended use of the product. For instance, it may be desirable to produce a finish with an "orange peel" texture when coating the doors of a refrigerator (to hide fingerprints), however, such a

finish is highly undesirable for the surface of an automobile hood. For a comprehensive study of chemical formulations and properties of coating materials used in the appliance and automotive industries, refer to [19] and [14], respectively. Basically, formulators of paint try to select properties of a paint's components to match the intended application. For instance, if a very smooth finish is desired, then resinous components are sought that atomize easily (for efficient spray application) and whose atomized droplets coalesce into continuous level films.

The hue of a surface that is coated with a colored paint depends (to a degree) on the film thickness of the paint. In particular, the film should be sufficiently thick so as to "hide" the influence of the color associated with the underlying primer coating (or the color of the surface itself if no primer coating is present). Thus, one way to produce a uniform hue across a surface is to accumulate a sufficient amount of film thickness at each surface point, i.e., enough thickness at each surface point to hide the primer. However, this approach can result in wasted paint if film thickness is not kept uniform across the surface. Also, those portions of the film that are too thick have the undesirable tendency to crack in use [17]. Thus, minimizing the variation in film thickness not only produces a more uniform hue across the entire surface, it also can also improve the "structural integrity" of the finish.

When painting hundreds or thousands of products per day, minimizing the amount of paint expended for each surface is important from both an environmental and an economical perspective. The United States automobile manufacturing industry expended over 183 million liters of paint to coat the 7.3 million passenger cars produced in 1983 (for an average of about 25 liters/car) [1]. Given the relative sensitivity and tightness of profit margins in the automotive industry, there is potential for increasing returns substantially with just a slight decrease in the amount of expended paint.

## ***B. Automated Spray Painting***

Robots are often used in large-scale production lines to position and/or move spray applicators around surfaces to be painted. To specify a trajectory for the robotic manipulator, it is common practice for an operator to literally "teach" the robot a path by grasping the end-effector and manually moving the end-effector around the part to be painted while the robot's control computer records position and orientation information [17]. Having stored the path information, the robot can then repeatedly traverse the "learned" path using a speed profile specified by the operator.

In this paper, the question of how to optimally traverse a spray applicator around a surface to be coated is formulated as a type of optimization problem known as a constrained variational problem. An optimal trajectory is defined here as one that results in minimal variation in film thickness on the surface. While other factors besides uniformity of film thickness also contribute to the overall quality of the finish, minimizing variation in film thickness is known to be a desirable property for many applications, see for example [2, 17].

The trajectory for an applicator is defined by a six-dimensional vector function that specifies the position and orientation of the applicator at each instant of time. The surface to be coated is assumed to be represented with a function. For each surface point and for each feasible position and orientation of the applicator, a value for the instantaneous rate of film accumulation is assumed to be known. Empirical data and/or estimates for these values can be readily incorporated in the formulation.

To illustrate why it is important to be able to incorporate empirical data for film accumulation rates, consider the utilization of electrostatic paint sprayers, which are heavily used in the automotive industry. Electrostatic painting is facilitated by charging atomized droplets of paint and using an electric field to enhance the transport of the drops to the work piece [20]. While the use of electrostatic painting can increase transfer

efficiency, it can also cause film to build in a nonuniform and/or nonintuitive manner. For example, a common effect known as "wrap-around" occurs when the lines of force (associated with the electric field) bend around the edges of the surface and cause droplets to be attracted to the edges and to the reverse side of a surface [17]. While this general effect is desirable for some applications, the precise nature of the effect is difficult to predict analytically because of the complicated interactions among the hydrodynamic, aerodynamic, and electrostatic forces on the particles of paint and the impact of the position and orientation of the applicator relative to the geometry of the surface.

From a practical viewpoint, it is desirable for a trajectory optimization technique to be able to utilize empirical data for film accumulation rates because such data can be obtained through off-line experimentation. For example, based on a representative collection of positions and orientations for the spray applicator relative to a given surface, corresponding film thickness measurements could be made to estimate the rate of film accumulation at each surface point. That is, film thickness measurement could be taken after spraying paint for a small (and known) amount of time from each feasible position and orientation. Both dry- and wet-film gauges can be used to measure film thickness. For a detailed description of such devices, refer to [17].

### *C. Organization of the Paper*

The remainder of the paper is organized in the following manner. In Section II, a model for the spray coating process is described and some associated notations are introduced. The mathematical formulation of the optimal trajectory planning problem is developed in Section III. In Section IV, solution techniques for the formulated optimization problem are developed for two classes of the assumed feasible set of applicator trajectories. Section V includes simulation studies that demonstrate the effectiveness of standard numerical techniques in providing solutions that achieve the desired objective. A summary and

some concluding remarks are included in the final section.

## II. MODELING AND NOTATION FOR SPRAY COATING

### A. The Surface Model

The object to be coated is assumed to be stationary and its location and surface geometry in three-dimensional euclidean space are described relative to a fixed reference frame  $\mathbf{XYZ}$ . The surface is assumed to be representable by a function  $z = h(x, y)$ , where the mapping  $h : \mathcal{D} \rightarrow \mathfrak{R}$  and its domain  $\mathcal{D} \subset \mathfrak{R}^2$  are specified. Applying standard set notation, the surface associated with the function  $h$  is defined as

$$\mathcal{S}_h = \{(x, y, z) : z = h(x, y), \text{ for all } (x, y) \in \mathcal{D}\}. \quad (1)$$

The assumption of having a functional representation for the surface of the object, i.e.,  $h(x, y)$ , is not unrealistic for many applications. For instance, in the automobile manufacturing industry, CAD models for surfaces are often a result of the design phase, and therefore a mathematical representation for the surface may already be known. There are several popular methods for representing geometric surfaces including the use of Coons/Ferguson patches, Bezier surfaces, and B-splines. For a more detailed description of these and other geometric modeling techniques, refer to [4, 15]. As it is not the intended thrust of the present paper to discuss how to convert various types of CAD models into the form  $z = h(x, y)$ , the existence of a function  $h(x, y)$  will henceforth be assumed with the realization that in practice some extra effort may be required for converting any particular CAD description into this form.

The assumption that each  $Z$  coordinate value on the surface is representable as an explicit function of its  $\mathbf{XY}$  coordinate values (i.e., that  $z = h(x, y)$ ) can be relaxed by making use of the implicit function theorem [8]. That is, the more general representation for a surface, which is to define surface points according to values that satisfy an equation

of the form  $s(x, y, z) = 0$ , where  $s : \mathbb{R}^3 \rightarrow \mathbb{R}$ , could be accommodated in the formulation. However, to do so unnecessarily complicates the notational burden without really adding new insight. Thus, without loss of generality, only surface geometries of the form  $z = h(x, y)$  are considered in this paper.

### B. *The Applicator Trajectory*

The spatial position and orientation of the applicator with respect to the fixed reference frame is defined by six values: three coordinate values for its position and three angular values for its orientation. These six values are defined at time  $t$  by a vector function:

$$\mathbf{a}(t) = [a_x(t) \ a_y(t) \ a_z(t) \ a_\psi(t) \ a_\theta(t) \ a_\phi(t)]'. \quad (2)$$

The values  $a_x(t)$ ,  $a_y(t)$ , and  $a_z(t)$  represent the applicator's position at time  $t$  with respect to the fixed euclidean reference frame XYZ. The values  $a_\psi(t)$ ,  $a_\theta(t)$ , and  $a_\phi(t)$ , describe the applicator's angular rotation with respect to the X, Y, and Z axes, respectively. This particular system of eulerian angles of rotation about the axes of the fixed reference frame is usually referred to as the "roll, pitch, and yaw" system. It is a simple matter to define a rotation matrix based on these angular values that can be used to transform the fixed reference frame to a rotated reference frame attached to the applicator [7].

### C. *The Rate of Film Accumulation*

In order to determine an optimal applicator trajectory for a given surface, information about the rate at which the film accumulates at each surface point (measured, for example, in  $\mu\text{m}/\text{sec}$ ) is assumed to be known. For the purposes of this paper, the rate at which film accumulates at each surface point is assumed to be dependent only on the geometry of the surface and the position and orientation of the applicator relative to the

surface. While the rate of film accumulation at each surface point is also a function of other parameters such as the flow rate of the coating material, the atomizing pressure, electrostatic voltage (if applicable), viscosity of the coating material, and solvent concentration, for the study here, these other parameter values will assumed to be fixed. Thus, only the interaction between the geometry of the surface and the position and orientation of the applicator will be considered in the formulation.

Let  $\dot{f}_{\mathcal{S}_h}(\mathbf{a}(t), x, y, t)$  denote the rate of film accumulation at time  $t$  at the point  $(x, y, h(x, y))$  on the surface  $\mathcal{S}_h$ , with the applicator trajectory defined by  $\mathbf{a}(t)$ . As the notation suggests, for a given surface  $\mathcal{S}_h$ , the rate of film accumulation at a point on the surface depends on the “ $x, y$ ” coordinates of the surface point and on time “ $t$ ,” which captures the position and orientation information for the applicator through the trajectory vector  $\mathbf{a}(t)$ . For the reasons indicated in the previous section, values for  $\dot{f}_{\mathcal{S}_h}(\mathbf{a}(t), x, y, t)$  may be derived from tabulated data (based on experimental measurements) and not necessarily expressed as an analytic function. An implicit assumption made here is that the rate of film accumulation does not explicitly depend on the velocity of the applicator, i.e.,  $\dot{\mathbf{a}}(t)$ . This is based on the practical presumption that the maximum feasible translational speed for the applicator is much smaller than the velocity of the paint droplets.

### III. THE OPTIMAL TRAJECTORY PLANNING PROBLEM

#### A. *The* Objective of the Optimal Trajectory Planning Problem

The objective of the optimal trajectory planning problem is to determine a trajectory that results in minimal variation in accumulated film thickness on the surface. The specific objective used here is the mean squared error between actual film thickness and average film thickness across the surface.

For a trajectory  $\mathbf{a}(t)$  defined over a time interval  $[0, T]$ , the film thickness accumulated

during the time interval  $[0, T]$  at each point  $(x, y, h(x, y))$  on the surface  $\mathcal{S}_h$  is given by

$$f_{\mathcal{S}_h}(\mathbf{a}(t), x, y) = \int_0^T \dot{f}_{\mathcal{S}_h}(\mathbf{a}(t), x, y, t) dt. \quad (3)$$

Due to the integration over time, the accumulated film thickness  $f_{\mathcal{S}_h}(\mathbf{a}(t), x, y)$  does not depend explicitly on  $t$ ; however, it does depend on the vector function  $\mathbf{a}(t)$ . The total volume of paint deposited onto the surface is given by

$$F_{\mathcal{S}_h}(\mathbf{a}(t)) = \iint_{\mathcal{D}} f_{\mathcal{S}_h}(\mathbf{a}(t), x, y) dx dy. \quad (4)$$

If the values for  $f_{\mathcal{S}_h}(\mathbf{a}(t), x, y, t)$  are derived from a collection experimentally measured data values and/or not expressed analytically, then the integration required in Eqs. (3) and (4) can be approximated numerically by using standard numerical integration techniques.

The area of the surface is given by [8]:

$$A_{\mathcal{S}_h} = \iint_{\mathcal{D}} \sqrt{1 + \left(\frac{\partial h}{\partial x}\right)^2 + \left(\frac{\partial h}{\partial y}\right)^2} dx dy, \quad (5)$$

where it is implicitly assumed that the functional description of the surface, i.e.,  $h(x, y)$ , can be partitioned into a finite number of smooth sub-surfaces. The average film thickness over the surface, denoted as  $f_{\mathcal{S}_h}^{\text{avg}}(\mathbf{a}(t))$ , is defined as the total volume of paint deposited onto the surface divided by the area of the surface:

$$f_{\mathcal{S}_h}^{\text{avg}}(\mathbf{a}(t)) = \left(\frac{1}{A_{\mathcal{S}_h}}\right) F_{\mathcal{S}_h}(\mathbf{a}(t)). \quad (6)$$

The variation in film thickness for the surface, denoted by  $V_{\mathcal{S}_h}(\mathbf{a}(t))$ , is defined as the mean squared error between film thickness at each point and average film thickness:

$$V_{\mathcal{S}_h}(\mathbf{a}(t)) = \frac{1}{A_{\mathcal{S}_h}} \iint_{\mathcal{D}} \left(f_{\mathcal{S}_h}(\mathbf{a}(t), x, y) - f_{\mathcal{S}_h}^{\text{avg}}(\mathbf{a}(t))\right)^2 dx dy. \quad (7)$$

The optimal trajectory problem involves finding a trajectory  $\mathbf{a}(t)$  that minimizes the variation in film thickness defined by Eq. (7).

### *B. Constraints for the Optimal Trajectory Planning Problem*

In practice, there are constraints on the set of trajectories that are feasible because of constraints associated with realistic robotic manipulators. In particular, there are constraints on the set of positions and orientations that are "reachable" by a given robotic system. Also, there are limits associated with the velocities and/or accelerations that can be developed to move the applicator along a reachable path.

In addition to the constraints imposed by the robotic manipulator itself, in practice it may be desirable to actually further constrain the collection of feasible trajectories. For instance, in some applications it may be practical to consider only those trajectories where the applicator's positions are within a range of distance (e.g., between 8 and 12 inches) from the surface and/or consider only orientations where the centerline of the applicator's spray pattern is normal to the surface. Adding such intuitive constraints decreases the size of the search space and may improve the quality of the obtained solution and/or increase the possibility of attaining a globally optimal solution.

Two classes of constraint sets for the assumed feasible trajectories are defined in the following two subsections. In the first, the desired spatial path for the trajectory is assumed to be specified. In the second, the spatial constraints for the trajectories are relaxed and thus the set of feasible trajectories is represented by a collection of six-dimensional vector functions of time.

### *C. The Optimal Trajectory Planning Problem Along a Specified Spatial Path*

A spatial point for an applicator is characterized by a six-dimensional vector that defines the position and orientation of the applicator. The spatial path associated with an applicator trajectory is defined as the set of spatial points traversed by the applicator. In some applications, a desired spatial path for the applicator may be specified. In such cases, the question of interest is how to best traverse the specified spatial path as a

function of time.

Let  $\mathbf{p}(\rho)$  denote a six-dimensional vector function that parameterizes a spatial path for the applicator. The scalar variable  $p \in [0, 1]$  parameterizes all points along the spatial path. Assume that the parameterization is such that  $\mathbf{p}(\rho)$  is a continuous function of the parameter  $p$ .

Consider a scalar function of time  $\lambda(t)$ , where  $\lambda : [0, T] \rightarrow [0, 1]$ . By replacing the scalar parameter  $p$  with the scalar function  $\lambda(t)$ , the resulting vector functional  $\mathbf{p}(\lambda(t))$  is a characterization of trajectories that have spatial points along the spatial path  $\mathbf{p}(\rho)$ . For practical reasons, it is generally necessary to constrain  $\lambda(t)$  to be a continuous function in order to prevent discontinuous movements of the applicator (recall that  $\mathbf{p}(\rho)$  is also assumed to be continuous in  $p$ ). It may further be necessary to limit the values of the first and/or second derivatives of  $\lambda(t)$  in order to constrain the speed and/or acceleration of the applicator. Finally, constraining  $\lambda(t)$  to be monotone increasing is tantamount to considering only those trajectories that do not backtrack along the specified spatial path. For notational convenience, the incorporation of all such desired constraints on  $\lambda(t)$  are assumed to be included in a set of scalar functions denoted by  $\Lambda(t)$ .

Thus, the optimal trajectory planning problem along a spatially parameterized path  $\mathbf{p}(\rho)$  is an optimization problem of the form

$$\min_{\lambda(t) \in \Lambda(t)} \{V_{S_h}(\mathbf{p}(\lambda(t)))\}. \quad (8)$$

The search space for the above optimization problem, i.e.,  $\Lambda(t)$ , is a set of scalar functions of time.

#### **D.** *The Optimal Trajectory Planning Problem With General Constraints*

In the general case, the feasible constraint set can include trajectories that do not share the same spatial path. Let  $\mathcal{A}(t)$  denote a general set of feasible applicator trajectories. Thus,  $\mathcal{A}(t)$  is a set of six-dimensional vector functions of time. In practice, the union of

all spatial points associated with all vector functions in  $\mathcal{A}(t)$  is constrained by the region that is reachable by the robotic manipulator. Also, the translational and/or rotational velocities of the trajectories in  $\mathcal{A}(t)$  may be constrained.

Therefore, the optimal trajectory planning problem with general constraints is an optimization problem of the form

$$\min_{\mathbf{a}(t) \in \mathcal{A}(t)} \{V_{S_h}(\mathbf{a}(t))\}. \quad (9)$$

In contrast to the optimal trajectory planning problem along a specified spatial path (where the search space is over a set of scalar functions of time) the optimization problem defined in Eq. (9) generically requires a search over a set of six-dimensional vector functions of time.

#### E. Classification of Optimal Trajectory Planning Problems

The optimal trajectory planning problem along a specified spatial path and the optimal trajectory planning problem with general constraints both belong to a general class of optimization problems known as constrained variational problems [6]. Constrained variational problems are analogous to, but more general than, problems that involve optimizing an ordinary function of several variables with constraints. Unlike the problem of optimizing an ordinary function  $f(\mathbf{x})$  over a constraint set  $\mathbf{X}$  (where the objective is to determine a vector  $\mathbf{x}^* \in \mathbf{X}$  such that  $f(\mathbf{x}^*) \leq f(\mathbf{x})$ , for all  $\mathbf{x} \in \mathbf{X}$ ) variational problems involve determining functions that minimize a given function of functions. Thus, in variational problems vector functions are sought that minimize a given functional. For the optimal trajectory planning problem of Eq. (8), a scalar function  $\lambda(t) \in \Lambda(t)$  is sought to minimize the functional  $V_{S_h}(\mathbf{p}(\lambda(t)))$ . For the optimal trajectory planning problem of Eq. (9), a vector function  $\mathbf{a}(t) \in \mathcal{A}(t)$  is sought to minimize the functional  $V_{S_h}(\mathbf{a}(t))$ .

Analogous to how an extremum for an ordinary function can be determined by setting the gradient of the function to zero, the extremum of a functional can be determined by

setting the "variation" of the functional to zero. While the precise definition for the variation of a functional shall not be given here (because it is not required for the solution techniques used in this paper) it is noted that an extremum function of a functional is the solution to a set of nonlinear differential equations that results from setting the variation of the functional to zero. Determining solutions for nonlinear differential equations is generally more complicated than determining solutions for the nonlinear algebraic equations associated with setting the gradient of an ordinary function to zero.

Because the differential equations associated with setting the variation of a functional to zero are easily integrated only in exceptional cases, other more practical approaches have been devised in the literature. One way to determine solutions to variational problems is to employ a so called direct method. The basic idea underlying direct methods is to consider a variational problem as a limit problem for some problem of extrema of a function of a finite number of variables [6]. The techniques described in the next section for solving the optimal trajectory problem are examples of direct methods.

#### IV. SOLUTION TECHNIQUES FOR OPTIMAL TRAJECTORY PLANNING PROBLEMS

##### A. Solving the Optimal Trajectory Planning Problem Along a Specified Spatial Path

The proposed technique for solving the optimization problem of Eq. (8) is based on approximating  $\lambda(t)$  as a piecewise constant function. Divide the interval  $[0, T]$  into  $N$  subintervals, each of width  $\Delta = T/N$ . Let  $b_k(t)$  denote a "boxcar" function, which is defined for each  $k \in [1, 2, \dots, N]$  as follows:

$$b_k(t) = \begin{cases} 1 & \text{if } t \in [(k-1)\Delta, k\Delta] \\ 0 & \text{otherwise.} \end{cases} \quad (10)$$

Thus, a piecewise constant approximation for  $\lambda(t)$  is given by

$$\tilde{\lambda}(t) = \sum_{k=1}^N \lambda_k b_k(t), \quad (11)$$

where  $\lambda_k \in [0, 1]$  represents the constant value of  $\tilde{\lambda}(t)$  over the subinterval  $[(k-1)\Delta, k\Delta]$ .

By replacing  $\mathbf{a}(t)$  with  $\mathbf{p}(\tilde{\lambda}(t))$  in the right side of Eq. (3), it is straightforward to verify the following expression for film thickness

$$\tilde{f}_{S_h}(\boldsymbol{\lambda}, x, y) = \Delta \sum_{k=1}^N \dot{f}_{S_h}(\mathbf{p}(\lambda_k), x, y), \quad (12)$$

where  $\boldsymbol{\lambda} = [\lambda_1 \ \lambda_2 \ \dots \ \lambda_N]^T$ .

Likewise, the corresponding expression for the variation in film thickness is given by

$$\tilde{V}_{S_h}(\boldsymbol{\lambda}) = \frac{1}{A_{S_h}} \iint_{\mathcal{D}} (\tilde{f}_{S_h}(\boldsymbol{\lambda}, x, y) - \tilde{f}_{S_h}^{\text{avg}}(\boldsymbol{\lambda}))^2 dx dy, \quad (13)$$

where

$$\tilde{f}_{S_h}^{\text{avg}}(\boldsymbol{\lambda}) = \frac{1}{A_{S_h}} \iint_{\mathcal{D}} \tilde{f}_{S_h}(\boldsymbol{\lambda}, x, y) dx dy. \quad (14)$$

The function  $\tilde{V}_{S_h}(\mathbf{A})$  represents an approximation to the functional objective associated with the original variational problem of Eq. (8). Of course the constraints on the allowable set of functions from the original variational problem, i.e.,  $\Lambda(t)$ , must also be transformed into a suitable constraint set for the vector  $\mathbf{A}$ . Clearly, the range of values for  $\lambda_k$  is bounded by  $0 \leq \lambda_k \leq 1$ , for all  $k \in [1, 2, \dots, N]$ . Also, in order to limit the speed among the feasible applicator trajectories, constraints may be placed on  $|\lambda_k - \lambda_{k+1}|$ , for each  $k \in [1, 2, \dots, N - 1]$ . Denote the set of vectors that include all such constraints on the vector  $\mathbf{A}$  by  $\mathbf{A}$ .

Thus, the nonlinear programming approximation to the optimal trajectory planning problem along a spatially parameterized path  $\mathbf{p}(\boldsymbol{\rho})$  has the form

$$\min_{\boldsymbol{\lambda} \in \mathbf{A}} \{\tilde{V}_{S_h}(\boldsymbol{\lambda})\}. \quad (15)$$

Provided that the function  $\tilde{V}_{S_h}(\boldsymbol{\lambda})$  is differentiable, then standard nonlinear programming techniques (e.g., gradient descent algorithms) can be employed to provide solutions to the optimization problem stated in Eq. (15) [3]. If the gradient of the objective function, i.e.,

$\nabla \tilde{V}_{S_h}(\boldsymbol{\lambda})$ , can not be expressed analytically, then it can be approximated numerically. An instance of this problem is solved in Section V by employing the quasi-Newton method with a finite-difference approximation for the gradient.

### B. Solving the Optimal Trajectory Planning Problem With General Constraints

Analogous to the technique of the previous subsection, the technique proposed here for solving the optimization problem of Eq. (9) is based on approximating  $\mathbf{a}(t)$  as a piecewise constant, vector function. Again, the interval  $[0, T]$  is divided into  $N$  subintervals, each of width  $\Delta = T/N$ . The boxcar function  $b_k(t)$  of Eq. (10) is used to define a piecewise constant approximation for  $\mathbf{a}(t)$ :

$$\hat{\mathbf{a}}(t) = \sum_{k=1}^N \mathbf{a}_k b_k(t), \quad (16)$$

where

$$\mathbf{a}_k = [a_{x,k} \ a_{y,k} \ a_{z,k} \ a_{\psi,k} \ a_{\theta,k} \ a_{\phi,k}]'. \quad (17)$$

Thus, the vector  $\mathbf{a}_k$  represents the position and orientation of the applicator during the time interval  $[(k-1)\Delta, k\Delta]$ .

By replacing  $\mathbf{a}(t)$  with  $\hat{\mathbf{a}}(t)$  in the right side of Eq. (3), it is straightforward to verify the following expression for film thickness

$$\hat{f}_{S_h}(\mathbf{a}, x, y) = \Delta \sum_{k=1}^N \dot{f}_{S_h}(\mathbf{a}_k, x, y), \quad (18)$$

where  $\mathbf{a} = [a'_1 \ a'_2 \ \dots \ a'_N]'$ .

Likewise, the corresponding expression for the variation in film thickness is given by

$$\hat{V}_{S_h}(\mathbf{a}) = \frac{1}{A_{S_h}} \iint_{\mathcal{D}} \left( \hat{f}_{S_h}(\mathbf{a}, x, y) - \hat{f}_{S_h}^{\text{avg}}(\mathbf{a}) \right)^2 dx dy, \quad (19)$$

where

$$\hat{f}_{S_h}^{\text{avg}}(\mathbf{a}) = \frac{1}{A_{S_h}} \iint_{\mathcal{D}} \hat{f}_{S_h}(\mathbf{a}, x, y) dx dy. \quad (20)$$

The function  $\widehat{V}_{S_h}(\mathbf{a})$  represents an approximation to the functional objective associated with the original variational problem of Eq. (9). In contrast to the analogous approximation given in Eq. (13), which depends on the N-vector  $\boldsymbol{\lambda}$ , the function  $\widehat{V}_{S_h}(\mathbf{a})$  generically depends on 6N variables because each of the N "components" of  $\mathbf{a}$ , i.e.,  $\mathbf{a}_k$ , is actually a six-dimensional vector.

The constraints on the feasible set of functions from the original variational problem, i.e.,  $\mathcal{A}(t)$ , must be transformed into a suitable constraint set for the vector  $\mathbf{a}$ . Clearly, the range of values for  $\mathbf{a}_k$  is bounded by the set of reachable spatial points of the robotic manipulator. Also, constraints may be placed on translational and rotational speeds by bounding  $[(a_{x,k} - a_{x,k+1})^2 + (a_{y,k} - a_{y,k+1})^2 + (a_{z,k} - a_{z,k+1})^2]^{\frac{1}{2}}$  and  $[(a_{\psi,k} - a_{\psi,k+1})^2 + (a_{\theta,k} - a_{\theta,k+1})^2 + (a_{\phi,k} - a_{\phi,k+1})^2]^{\frac{1}{2}}$ , respectively. Denote the set of vectors that include all such constraints on  $\mathbf{a}$  by  $\mathbf{A}$ .

Thus, the nonlinear programming approximation to the optimal trajectory planning problem with general constraints has the form

$$\min_{\mathbf{a} \in \mathbf{A}} \{ \widehat{V}_{S_h}(\mathbf{a}) \}. \quad (21)$$

Analogous to the discussion of practical solution techniques for the optimization problem of Eq. (15), if that the function  $\widehat{V}_{S_h}(\mathbf{a})$  is sufficiently smooth (i.e., differentiable), then standard nonlinear programming techniques can also be employed to provide solutions to optimization problem of Eq. (21).

## V. NUMERICAL RESULTS

The optimization technique proposed in Section IV.A (for traversing a specified spatial path) is evaluated here for a particular example problem.

### A. Problem Setup

The surface to be painted is a square flat panel that is located within the  $XY$  plane. The four corners of the panel are positioned at the  $XY$  coordinates  $(1\frac{1}{3}, 0)$ ,  $(1\frac{1}{3}, 5\frac{1}{3})$ ,  $(6\frac{2}{3}, 5\frac{1}{3})$ , and  $(6\frac{2}{3}, 0)$ . Using the notation of Eq. (1), the surface of the panel is denoted by  $\mathcal{S}_0 = \{(x, y, 0) : 1\frac{1}{3} \leq x \leq 6\frac{2}{3} \ \& \ 0 \leq y \leq 5\frac{1}{3}\}$ .

It is assumed that the applicator can be positioned above the panel so that the centerline of the spray pattern is oriented normal to the panel's surface. This could be achieved, for example, with a cartesian-type robot having three linear axes of motion aligned with the fixed reference frame. Only the  $X$  and  $Y$  coordinates of the applicator are controlled; the  $Z$  coordinate of the applicator is assumed to be constant and has a value of unity. The angular values that define the orientation of the applicator with respect to the three axes of the reference frame are fixed and have values of zero. Thus, the assumed trajectory for the applicator is of the form

$$\mathbf{a}(t) = [a_x(t) \ a_y(t) \ 1 \ 0 \ 0 \ 0]'. \quad (22)$$

For each surface point  $(x, y, 0) \in \mathcal{S}_0$ , the assumed rate of film rate accumulation is given by

$$\dot{f}_{\mathcal{S}_0}(\mathbf{a}(t), x, y, t) = \frac{1}{(1 + (x - a_x(t))^2)(1 + (y - a_y(t))^2)}. \quad (23)$$

For each value of time  $t$ , the above function is a scaled bivariate Cauchy density function centered at the  $XY$  coordinate  $(a_x(t), a_y(t))$  [13]. The spread parameters along the  $X$  and  $Y$  axes are assumed to be unity. From the formula, note that the maximum rate of film accumulation occurs at the  $XY$  coordinate where  $x = a_x(t)$  and  $y = a_y(t)$ , i.e., at the  $XY$  coordinate directly under the applicator. This is consistent with the characteristics of many realistic applicators, which often have a "bell-shaped" distribution for the density of paint particles [12]. One advantage of the assumed formula of Eq. (23) is that its integral over the assumed surface (i.e., a flat panel) can be expressed as an analytic

function. In practice, empirical data and/or estimates for values of  $\dot{f}_{S_0}(\mathbf{a}(t), x, \mathbf{y}, t)$  can be used and the required integration can be carried out numerically.

For convenience, the units of length are not specified here. In practice, the units for the dimensions of the panel may be on the order of a few feet or meters and the units for the rate of film accumulation could be on the order of a  $\mu\text{m}/\text{sec}$ .

Fig. 1 shows the XY coordinates of a parameterized spatial path denoted by  $\mathbf{p}_{\ell,d}(\rho)$ . The value of  $\ell$  is the length of each straight segment associated with the four horizontal "sweeps" over the panel and  $d$  is the indexing distance between consecutive sweeps. The end-points of the horizontal segments are connected by semicircular arcs of radius  $\frac{d}{2}$ . The total length of the path is given by  $L = 4\ell + \frac{3\pi d}{2}$ . A analytical parameterization of the path of the form  $\mathbf{p}_{\ell,d}(\rho) = [p_x(\rho) \ p_y(\rho) \ 1 \ 0 \ 0 \ 0]'$ ,  $\rho \in [0, 1]$ , is given in Appendix A.

### B. *Traversing* the Assumed Spatial Path at a Constant Speed

The type of parameterization given in Appendix A for the path  $\mathbf{p}_{\ell,d}(\rho)$  is known as a parameterization by arc length, which means that a unit change in the parameterizing variable  $\rho$  results in a unit change in curve length along the path [9]. It is straightforward to verify this property by noting that  $((\frac{\partial p_x(\rho)}{\partial \rho})^2 + (\frac{\partial p_y(\rho)}{\partial \rho})^2)^{\frac{1}{2}} = L$ , for all  $\rho \in [0, 1]$ . Thus, trajectories of the form  $\mathbf{p}_{\ell,d}(\frac{1}{T}t)$ , for  $t \in [0, T]$ , represent a constant speed traversal of the spatial path  $\mathbf{p}_{\ell,d}(\rho)$  over the time interval  $[0, T]$ .

Let  $\tilde{\lambda}_{T,N}^{\text{lin}}(t)$  denote a piecewise constant approximation to a linearly increasing function of time, which is defined for each  $t \in [0, T]$  by

$$\tilde{\lambda}_{T,N}^{\text{lin}}(t) = \sum_{k=1}^N \left( k - \frac{0.5}{N} \right) \Delta b_k(t), \quad (24)$$

where  $\Delta = T/N$  and the  $b_k(t)$  is the boxcar function as defined by Eq. (10). A plot of  $\tilde{\lambda}_{T,N}^{\text{lin}}(t)$  is shown in Fig. 2a for the case  $T = 10.57$  and  $N = 100$ . Let  $\boldsymbol{\lambda}_{T,N}^{\text{lin}}$  denote the N-vector whose components are the coefficients of the piecewise constant function  $\tilde{\lambda}_{T,N}^{\text{lin}}(t)$ , i.e., the  $k$ th component of  $\boldsymbol{\lambda}$  is  $(k - \frac{0.5}{N})\Delta$ .

The  $XY$  coordinates of the trajectory  $\mathbf{p}_{\ell,d}(\tilde{\lambda}_{T,N}^{\text{lin}}(t))$  is represented graphically in Fig. 2b for the case  $\ell = 8$ ,  $d = 1\frac{7}{9}$ ,  $T = 10.57$  and  $N = 100$ . The panel is indicated by the shaded area. There are 100 “\*” symbols along the spatial path, which indicate the applicator's position during the consecutive time intervals of width  $A = TIN = 0.1057$ . The fact that the “\*” symbols are evenly spaced indicates that the applicator moves at a constant speed along the spatial path (as expected). Fig. 2c shows a contour plot for the panel's film thickness, which is a result of the trajectory of Fig. 2b.

A plot of  $\tilde{\lambda}_{T,N}^{\text{lin}}(t)$  is shown in Fig. 3a for the case  $T = 8.34$  and  $N = 74$ . Fig. 3b shows the  $XY$  coordinates of the trajectory defined by  $\mathbf{p}_{\ell,d}(\tilde{\lambda}_{T,N}^{\text{lin}}(t)) + [1\frac{1}{3} \ 0 \ \dots \ 0]'$  for the case  $\ell = 5\frac{1}{3}$ ,  $d = 1\frac{7}{9}$ ,  $T = 8.34$ , and  $N = 74$ . The 74 evenly spaced “\*” symbols indicate the applicator's position during consecutive time intervals of width  $A = TIN = 0.1127$ . Fig. 3c shows a contour plot for the panel's film thickness, which is a result of the constant speed trajectory of Fig. 3b.

Even though the total time duration  $T$  for the trajectories of Fig. 2b and Fig. 3b are distinct (i.e., 10.57 and 8.34, respectively) the average film thickness for the associated contour plots of Fig. 2c and Fig. 3c are equal (and have a value of unity). From the contour plots, it is apparent that the surface profile of Fig. 2c has less variation than that of Fig. 3c. The trajectory of Fig. 2b expends 27% more paint than that of Fig. 3b, because the duration of the spraying time for the trajectory of Fig. 2b (i.e.,  $T = 10.57$ ) is 27% longer than that of Fig. 3b (i.e.,  $T = 8.34$ ). This is not surprising because a relatively large fraction of the spatial path in Fig. 2b is not positioned directly over the panel (which also explains why more spraying time is required for the trajectory of Fig. 2b to accumulate the same average thickness of paint on the surface). Thus, by increasing the length of each sweep (i.e., increasing the value of  $\ell$ ) the variation in film thickness is decreased; however, the total painting time and the total amount of paint expended to accumulate the same average thickness on the surface is increased.

### C. Optimal Traversal of a Specified Spatial Path

In this subsection, the optimization technique of Section IV.A is applied to the spatial path  $\mathbf{p}_{\ell,d}(\rho) + [1\frac{1}{3} \ 0 \ \dots \ 0]'$  with  $\ell = 5\frac{1}{3}$  and  $d = 1\frac{7}{9}$  (same as the spatial path assumed in Fig. 3b). The values  $N = 74$  and  $\mathbf{T} = 9.37$  are used to define the piecewise constant function,  $\tilde{\lambda}(t)$  of Eq. (11). The nonlinear function to be minimized, denoted below as  $\tilde{V}_{S_0}(\boldsymbol{\lambda})$ , is derived in Appendix B.

$$\begin{aligned}
\tilde{V}_{S_0}(\boldsymbol{\lambda}) = & \frac{\Delta^2}{A_{S_0}} \left( \sum_{k=1}^N \left( \frac{x - p_{xk}}{2 + 2(x - p_{xk})^2} + \frac{1}{2} \tan^{-1}(x - p_{xk}) \right) \Big|_{\underline{x}}^{\bar{x}} \right. \\
& \left. \left( \frac{y - p_{yk}}{2 + 2(y - p_{yk})^2} + \frac{1}{2} \tan^{-1}(y - p_{yk}) \right) \Big|_{\underline{y}}^{\bar{y}} \right) \\
& + 2 \sum_{i=1}^{N-1} \sum_{j=i+1}^N \\
& \left( \frac{-\ln(1 + x^2 - 2xp_{xi} + p_{xi}^2) + (p_{xj} - p_{xi})\tan^{-1}(p_{xj} - x)}{4p_{xi} - 4p_{xj} - p_{xj}^3 + 3p_{xi}p_{xj}^2 - 3p_{xj}p_{xi}^2 + p_{xi}^3} \right. \\
& \left. + \frac{\ln(1 + x^2 - 2xp_{xj} + p_{xj}^2) + (p_{xj} - p_{xi})\tan^{-1}(p_{xj} - x)}{4p_{xi} - 4p_{xj} - p_{xj}^3 + 3p_{xi}p_{xj}^2 - 3p_{xj}p_{xi}^2 + p_{xi}^3} \right) \Big|_{\underline{x}}^{\bar{x}} \\
& \left( \frac{-\ln(1 + y^2 - 2yp_{yi} + p_{yi}^2) + (p_{yj} - p_{yi})\tan^{-1}(p_{yj} - y)}{4p_{yi} - 4p_{yj} - p_{yj}^3 + 3p_{yi}p_{yj}^2 - 3p_{yj}p_{yi}^2 + p_{yi}^3} \right. \\
& \left. + \frac{\ln(1 + y^2 - 2yp_{yj} + p_{yj}^2) + (p_{yj} - p_{yi})\tan^{-1}(p_{yj} - y)}{4p_{yi} - 4p_{yj} - p_{yj}^3 + 3p_{yi}p_{yj}^2 - 3p_{yj}p_{yi}^2 + p_{yi}^3} \right) \Big|_{\underline{y}}^{\bar{y}} \\
& - \left( \frac{\Delta}{A_{S_0}} \sum_{k=1}^N \left( \tan^{-1}(x - p_{xk}) \right) \Big|_{\underline{x}}^{\bar{x}} \left( \tan^{-1}(y - p_{yk}) \right) \Big|_{\underline{y}}^{\bar{y}} \right)^2, \tag{25}
\end{aligned}$$

where  $p_{xk}$  and  $p_{yk}$  denote  $p_x(\lambda_k)$  and  $p_y(\lambda_k)$ , respectively; the four corners of the panel have  $XY$  coordinates  $(\underline{x}, \underline{y})$ ,  $(\underline{x}, \bar{y})$ ,  $(\bar{x}, \underline{y})$ , and  $(\bar{x}, \bar{y})$ ; and the area of the surface is given by  $A_{S_0} := (\bar{x} - \underline{x})(\bar{y} - \underline{y})$ .

The assumed constraint set for A is defined by

$$\mathbf{A} = \{\boldsymbol{\lambda} = [\lambda_1 \dots \lambda_N]': 0 \leq \lambda_i \leq 1\}. \tag{26}$$

The nonlinear optimization problem of minimizing the function  $\tilde{V}_{S_0}(\mathbf{A})$  of Eq. (25) subject to the constraint set  $\mathbf{A}$  of Eq. (26) was solved using an IMSL subroutine. The

particular subroutine employed was BCONF, which uses a quasi-Newton method and a finite-difference gradient to minimize nonlinear functions with simple bounds on the variables [10]. The vector  $\boldsymbol{\lambda}_{T,N}^{\text{lin}}$  with  $T = 9.37$  and  $N = 74$  was used as the initial condition for the algorithm. The default convergence parameters were used for the BCONF subroutine and the solution was obtained after about one hour of cpu time on a Sun Sparcstation 1.

Because the value of the objective function  $\tilde{V}_{S_0}(\boldsymbol{\lambda})$  is independent of how the components of the vector  $\mathbf{A}$  are permuted, the obtained optimal piecewise constant function, denoted by  $\tilde{\lambda}^*(t)$ , is defined with the components of the solution vector  $\mathbf{A}^*$  sorted in ascending order. A plot of the optimal piecewise constant function  $\tilde{\lambda}^*(t)$  is shown in Fig. 4a. Fig. 4b shows the 74 positions of the applicator based on the optimal solution  $\tilde{\lambda}^*(t)$  of Fig. 4a (which has an assumed time step  $\Delta t = T/N = 0.1266$ ). Fig. 4c shows a contour plot for the panel's film thickness, which is a result of the optimal trajectory of Fig. 4b.

Table I gives the performance features of the three trajectories described in Figs. 2, 3, and 4. To summarize these results, the optimal trajectory of Fig. 4 delivers a mean squared error that is about three times smaller than that of Fig. 2 and more than five times smaller than that of Fig. 3. Also, the total painting time (which is proportional to the amount of expended paint) for the optimal trajectory is about 13% less than the trajectory of Fig. 2a and 12% more than the trajectory of Fig. 3a.

Fig. 5a shows the result of smoothing the piecewise constant function  $\tilde{\lambda}^*(t)$  with a cubic spline [4]. The trajectory associated with sampling  $N = 740$  values from the smoothed curve (ten times more resolution than the original sampling) over a period of  $T = 9.37$  seconds is shown in Fig. 5b. Fig. 5c shows the contour plot for film thickness that results from the sampled smooth trajectory of Fig. 5b. The mean squared error for the contour plot of Fig. 5c is 0.001933, which is only slightly greater than the mean

TABLE I. SIMULATION RESULTS

Graphical Views (trajectory type)	$\mathbf{p}_{\ell,d}(\rho)$		$\tilde{\lambda}(t)$		$\tilde{f}_{S_0}^{\text{avg}}(\boldsymbol{\lambda})$	$\tilde{V}_{S_0}(\boldsymbol{\lambda})$
	$\ell$	$d$	$N$	$T$		
Fig. 2 (constant speed)	8	$1\frac{7}{9}$	100	10.57	1.00	0.004591
Fig. 3 (constant speed)	5	$1\frac{7}{9}$	74	8.34	1.00	0.008714
Fig. 4 (optimal)	5	$1\frac{7}{9}$	74	9.37	1.00	<b>0.001692</b>
Fig. 5 (smoothed optimal)	5	$1\frac{7}{9}$	740	9.37	1.00	<b>0.001933</b>

squared error of 0.001692 associated with the optimal piecewise constant trajectory of Fig. 4.

## VI. CONCLUSIONS

A framework for solving an optimal trajectory planning problem for spray coating was developed. The proposed methodology is general in the sense that no real limitations are placed on the spray coating system nor the surface to be coated. The methodology can utilize empirically-based information for the rate film accumulation at each surface point, as a function of the position and orientation of the applicator. It was demonstrated through an example that standard commercially available nonlinear programming algorithms can be applied to solve the formulated optimization problem.

Future work will include utilizing the techniques developed here as the basis for an interactive and graphically-based tool for trajectory planning. A similar tool for this purpose was developed in [21]. However, in [21] the assumed spray pattern is circular and the rate of film accumulation within the circular pattern is assumed to be uniform. Thus, our more general formulation may provide a more realistic basis for simulation and

optimization.

The optimal trajectory planning problem with general constraints (i.e., where both the spatial and temporal components of the trajectory are sought) may prove to be computationally intractable because of the complexity of the constraint set. In practice, an approach that allows the operator to specify the spatial path and uses the proposed optimization technique to determine how to traverse the path as a function of time shows great promise. A graphically-based tool would enable the operator to evaluate the merit of several trajectories through off-line simulation. As the simulation studies done in this paper indicate, the best way to traverse a simple spatial path over a flat panel is not entirely intuitive.

#### ACKNOWLEDGMENTS

The author thanks Ting-Li Ling, Ramanujam Ramabhadran, and Simon P. Yeung for their assistance in developing the software for the simulation studies.

#### APPENDIX A

An analytic parameterization of the spatial path shown in Fig. 1 is derived in this appendix. The parameterization is of the form  $\mathbf{p}_{\ell,d}(\rho) = [p_x(\rho) \ p_y(\rho) \ 1 \ 0 \ 0 \ 0]'$ ,  $\rho \in [0,1]$ . The length of the path is denoted by  $L = 4l + \frac{3\pi d}{2}$ . The expressions for  $p_x(\rho)$  and  $p_y(\rho)$  are defined by partitioning the interval  $[0, 1]$  for  $\rho$  into seven subintervals: as follows:

- if  $(0 \leq \rho < \frac{1}{L}l)$

$$p_x(\rho) = L\rho$$

$$p_y(\rho) = 3d$$

- if  $(\frac{1}{L}\ell \leq \rho < \frac{1}{L}(\ell + \frac{\pi d}{2}))$ 

$$p_x(\rho) = e + \frac{d}{2} \cos[(\frac{1}{L}\ell - \rho)\frac{2L}{d} + \frac{\pi}{2}]$$

$$p_y(\rho) = \frac{5d}{2} + \frac{d}{2} \sin[(\frac{1}{L}\ell - \rho)\frac{2L}{d} + \frac{\pi}{2}]$$
- if  $(\frac{1}{L}(\ell + \frac{\pi d}{2}) \leq \rho < \frac{1}{L}(2\ell + \frac{\pi d}{2}))$ 

$$p_x(\rho) = 2e + \frac{\pi d}{2} - L\rho$$

$$p_y(\rho) = 2d$$
- if  $(\frac{1}{L}(2\ell + \frac{\pi d}{2}) \leq \rho < \frac{1}{L}(2\ell + \pi d))$ 

$$p_x(\rho) = \frac{d}{2} \cos[\frac{2L}{d}(\rho - \frac{1}{L}(2\ell + \frac{\pi d}{2})) + \frac{\pi}{2}]$$

$$p_y(\rho) = \frac{3d}{2} + \frac{d}{2} \sin[\frac{2L}{d}(\rho - \frac{1}{L}(2\ell + \frac{\pi d}{2})) + \frac{\pi}{2}]$$
- if  $(\frac{1}{L}(2\ell + \pi d) \leq \rho < \frac{1}{L}(3\ell + \pi d))$ 

$$p_x(\rho) = L\rho - 2e - \pi d$$

$$p_y(\rho) = d$$
- if  $(\frac{1}{L}(3\ell + \pi d) \leq \rho < \frac{1}{L}(3\ell + \frac{3\pi d}{2}))$ 

$$p_x(\rho) = \ell + \frac{d}{2} \cos[(\frac{1}{L}(3\ell + \pi d) - \rho)\frac{2L}{d} + \frac{\pi}{2}]$$

$$p_y(\rho) = \frac{d}{2} + \frac{d}{2} \sin[(\frac{1}{L}(3\ell + \pi d) - \rho)\frac{2L}{d} + \frac{\pi}{2}]$$
- if  $(\frac{1}{L}(3\ell + \frac{3\pi d}{2}) \leq \rho < \frac{1}{L}(4\ell + \frac{3\pi d}{2}) = 1)$ 

$$p_x(\rho) = 4e + \frac{3\pi d}{2} - L\rho$$

$$p_y(\rho) = 0.$$

## APPENDIX B

The analytical expression for the objective function  $\tilde{V}_{S_0}(\boldsymbol{\lambda})$  of Eq. (25) is derived in this appendix. From Eq.(13), it is straightforward to verify the following alternate general

expression for  $\tilde{V}_{S_h}(A)$ :

$$\tilde{V}_{S_h}(\boldsymbol{\lambda}) = \frac{1}{A_{S_h}} \iint_{\mathcal{D}} (\tilde{f}_{S_h}(\boldsymbol{\lambda}, x, y))^2 dx dy - (\tilde{f}_{S_h}^{\text{avg}}(\boldsymbol{\lambda}))^2. \quad (B.1)$$

By evaluating Eq. (12) using the assumed formula for the rate of film accumulation given in Eq. (23), the expression for film thickness on the surface  $\mathcal{S}_0$  is given by

$$\tilde{f}_{S_0}(\boldsymbol{\lambda}, x, y) = \Delta \sum_{k=1}^N \frac{1}{(1 + (x - p_{xk})^2)(1 + (y - p_{yk})^2)}, \quad (B.2)$$

where  $p_{xk}$  and  $p_{yk}$  denote  $p_x(\lambda_k)$  and  $p_y(\lambda_k)$ , respectively. The analytic parameterization of the assumed spatial path coordinates  $p_x(\cdot)$  and  $p_y(\cdot)$  are given in Appendix A.

By denoting the XY coordinates for the four corners of the panel as  $(\underline{x}, \underline{y})$ ,  $(\underline{x}, \bar{y})$ ,  $(\bar{x}, \bar{y})$ , and  $(\bar{x}, \underline{y})$ , the expression for average film thickness is given by

$$\tilde{f}_{S_0}^{\text{avg}}(\boldsymbol{\lambda}) = \frac{1}{A_{S_0}} \int_{\underline{y}}^{\bar{y}} \int_{\underline{x}}^{\bar{x}} \Delta \sum_{k=1}^N \frac{1}{(1 + (x - p_{xk})^2)(1 + (y - p_{yk})^2)} dx dy, \quad (B.3)$$

where

$$A_{S_0} = (\bar{y} - \underline{y})(\bar{x} - \underline{x}). \quad (B.4)$$

Exchanging the order of summation and integration and evaluating the integrals of Eq. (B.3) gives

$$\begin{aligned} \tilde{f}_{S_0}^{\text{avg}}(\boldsymbol{\lambda}) &= \frac{\Delta}{A_{S_0}} \sum_{k=1}^N \left( \tan^{-1}(x - p_{xk}) \right) \Big|_{\underline{x}}^{\bar{x}} \left( \tan^{-1}(y - p_{yk}) \right) \Big|_{\underline{y}}^{\bar{y}} \\ &= \frac{\Delta}{A_{S_0}} \sum_{k=1}^N \left( \tan^{-1}(\bar{x} - p_{xk}) - \tan^{-1}(\underline{x} - p_{xk}) \right) \\ &\quad \left( \tan^{-1}(\bar{y} - p_{yk}) - \tan^{-1}(\underline{y} - p_{yk}) \right). \end{aligned} \quad (B.5)$$

Let  $\mathbf{I}$  denote the first term of Eq. (B.1), i.e., the integral term. The value of  $\mathbf{I}$  is determined for the surface  $\mathcal{S}_0$  by first squaring and then integrating the expression for  $\tilde{f}_{S_0}(\boldsymbol{\lambda}, x, y)$  of Eq. (B.2):

$$I = \frac{1}{A_{S_0}} \int_{\underline{y}}^{\bar{y}} \int_{\underline{x}}^{\bar{x}} \left( \Delta \sum_{k=1}^N \frac{1}{(1 + (x - p_{xk})^2)(1 + (y - p_{yk})^2)} \right)^2 dx dy$$

$$\begin{aligned}
&= \frac{\Delta^2}{A_{S_0}} \left( \sum_{k=1}^N \left( \frac{x - p_{xk}}{2 + 2(x - p_{xk})^2} + \frac{1}{2} \tan^{-1}(x - p_{xk}) \right) \Big|_{\underline{x}}^{\bar{x}} \right. \\
&\quad \left. \left( \frac{y - p_{yk}}{2 + 2(y - p_{yk})^2} + \frac{1}{2} \tan^{-1}(y - p_{yk}) \right) \Big|_{\underline{y}}^{\bar{y}} \right) \\
&\quad - 2 \sum_{i=1}^{N-1} \sum_{j=i+1}^N \\
&\quad \left( \frac{-\ln(1 + x^2 - 2xp_{xi} + p_{xi}^2) + (p_{xj} - p_{xi})\tan^{-1}(p_{xj} - x)}{4p_{xi} - 4p_{xj} - p_{xj}^3 + 3p_{xi}p_{xj}^2 - 3p_{xj}p_{xi}^2 + p_{xi}^3} \right. \\
&\quad \left. + \frac{\ln(1 + x^2 - 2xp_{xj} + p_{xj}^2) + (p_{xj} - p_{xi})\tan^{-1}(p_{xj} - x)}{4p_{xi} - 4p_{xj} - p_{xj}^3 + 3p_{xi}p_{xj}^2 - 3p_{xj}p_{xi}^2 + p_{xi}^3} \right) \Big|_{\underline{x}}^{\bar{x}} \\
&\quad \left( \frac{-\ln(1 + y^2 - 2yp_{yi} + p_{yi}^2) + (p_{yj} - p_{yi})\tan^{-1}(p_{yj} - y)}{4p_{yi} - 4p_{yj} - p_{yj}^3 + 3p_{yi}p_{yj}^2 - 3p_{yj}p_{yi}^2 + p_{yi}^3} \right. \\
&\quad \left. + \frac{\ln(1 + y^2 - 2yp_{yj} + p_{yj}^2) + (p_{yj} - p_{yi})\tan^{-1}(p_{yj} - y)}{4p_{yi} - 4p_{yj} - p_{yj}^3 + 3p_{yi}p_{yj}^2 - 3p_{yj}p_{yi}^2 + p_{yi}^3} \right) \Big|_{\underline{y}}^{\bar{y}} \Big). \tag{B.6}
\end{aligned}$$

Thus, the assumed objective function is

$$\tilde{V}_{S_0}(\boldsymbol{\lambda}) = I - \left( \tilde{f}_{S_0}^{\text{avg}}(\boldsymbol{\lambda}) \right)^2, \tag{B.7}$$

where  $I$  and  $\tilde{f}_{S_0}^{\text{avg}}(\boldsymbol{\lambda})$  are given in Eqs. (B.6) and (B.5), respectively.

## REFERENCES

- [1] D. A. Ansdell, "Automotive paints," in *Paint and Surface Coatings: Theory and Practice*, edited by R. Lambourne, John Wiley & Sons, New York, NY, 1987, pp. 431–489.
- [2] J. K. Antonio, J. G. Wendelberger, G. P. Matthews, W. G. Trabold, and M. H. Costin, "Optiscan: the use of reflectometry for detecting quality attributes of basecoat paint," General Motors Research Laboratories, Warren, MI, Research Report No. ET-426/MA-357, Dec. 1986.

- [3] M. S. Bazaraa, H. D. Sherali, and C. M. Shetty, *Nonlinear Programming: Theory and Algorithms*, Second Edition, John Wiley & Sons, New York, NY, 1993.
- [4] C. de Boor, *A Practical Guide to Splines*, Applied Mathematical Sciences Series, vol. 27, Springer-Verlag, New York, NY, 1978.
- [5] D. Dobson, "Leading edge robotic finishing technologies," Society of Manufacturing Engineers, Dearborn MI, Technical Paper MS89-136, 1989.
- [6] L. E. Elsgolc, *Calculus of Variations*, Addison-Wesley, Reading, MA, 1962.
- [7] K. S. Fu, R. C. Gonzalez, and C. S. G. Lee, *Robotics: Control, Sensing, Vision, and Intelligence*, McGraw-Hill, New York, NY, 1987.
- [8] W. Fulks, *Advanced Calculus*, Third Edition, John Wiley & Sons, New York, NY, 1958.
- [9] B. Guenter and R. Parent, "Computing the arc length of parametric curves," *IEEE Computer Graphics & Applications*, May 1990, pp. 72–78.
- [10] IMSL Math-Library, Version 1.1, Volume 3, IMSL Corporation, Houston, TX, Jan. 1989, pp. 847–852.
- [11] H. H. Kuo and J. G. Wendelberger, "GM-ORACLE II: computer simulation of paint spray patterns," General Motors Research Laboratories, Warren, MI, Research Report No. PO-769, Apr. 1986.
- [12] A. H. Lefebvre, *Atomization and Sprays*, Hemisphere Publishing, New York, NY, 1989.
- [13] A. M. Mood, F. A. Graybill, and D. C. Boes, *Introduction to the Theory of Statistics*, Third Edition, McGraw-Hill, New York, NY, 1974.

- [14] B. N. McBane, "Automotive coatings," in *Treatise on Coatings, Volume 4, Formulations, Part I*, edited by R. R. Myers and J. S. Long, Marcel Dekker, New York, NY, 1975, pp. 153–232.
- [15] M. Mortenson, *Geometric Modeling*, John Wiley & Sons, New York, NY, 1985.
- [16] S. Paul, *Surface Coatings*, John Wiley & Sons, New York, NY, 1985.
- [17] G. L. Schneberger, *Understanding Paint and Painting Processes, Fourth Edition*, Hitchcock Publishing, Carol Stream, IL, 1989.
- [18] F. Scofield, "Status of air pollution control regulations," in *Nonpolluting Coatings and Coating Processes*, edited by J. L. Gardon and J. W. Prane, Plenum Press, New York, NY, 1973, pp. 1–3.
- [19] E. G. Shur, "Appliance finishes," in *Treatise on Coatings, Volume 4, Formulations, Part I*, edited by R. R. Myers and J. S. Long, Marcel Dekker, New York, NY, 1975, pp. 85–152.
- [20] H. E. Snyder, D. W. Senser, A. H. Lefebvre, and R. S. Coutinho, "Drop size measurements in electrostatic paint sprays," *IEEE Trans. Industry Applications*, vol. 25, no. 4, July/August 1989, pp. 720–727.
- [21] S.-H. Suh, I.-K. Woo, and S.-K. Noh, "Development of an automatic trajectory planning system (ATPS) for spray painting robots," *Proc. 1991 IEEE Int'l Conference on Robotics and Automation*, April 1991, pp. 1948–1955.

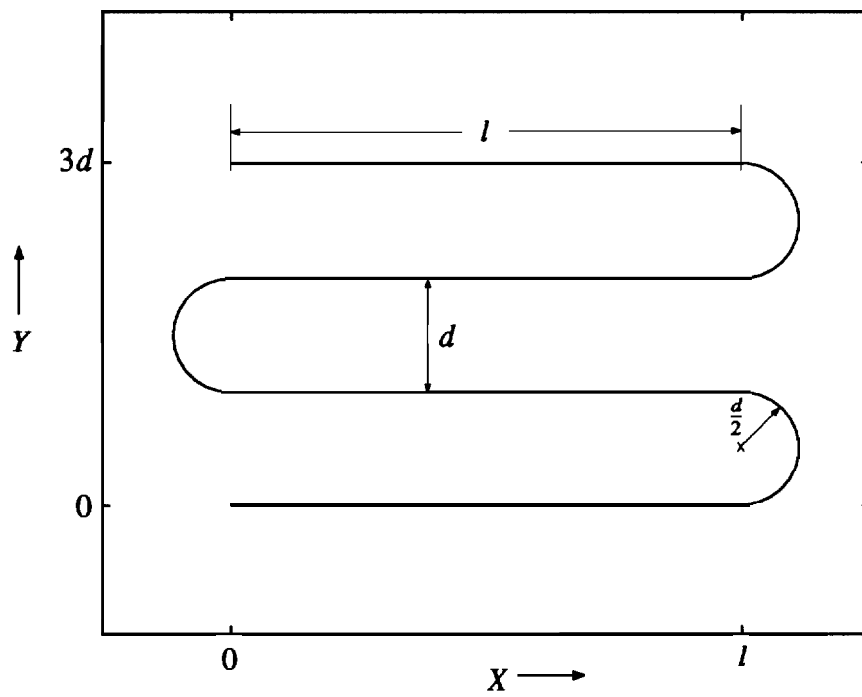


Fig. 1. The XY coordinates of the parameterized spatial path  $\mathbf{p}_{\ell,d}(\rho)$ .

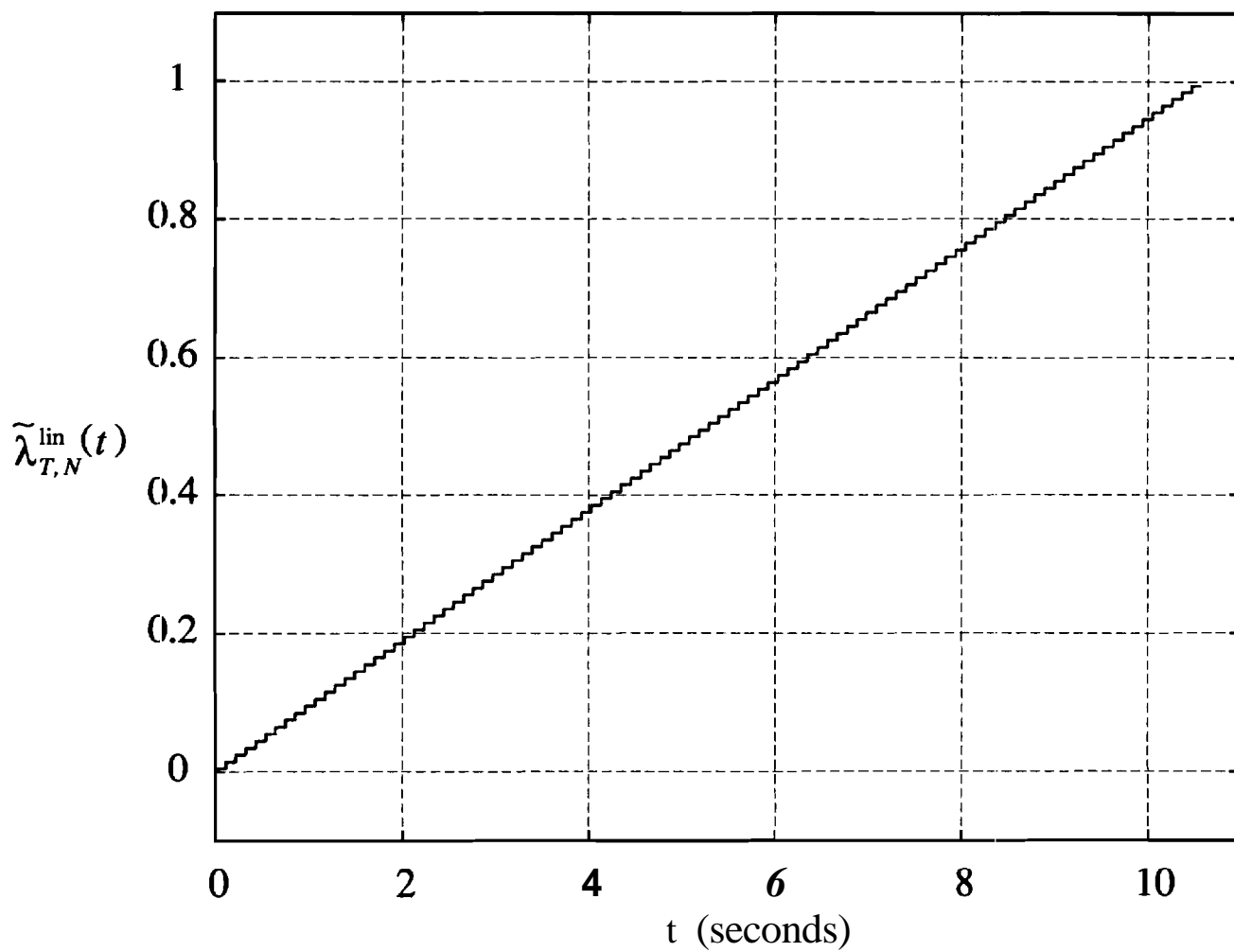


Fig. 2a. A piecewise constant approximation to a linearly increasing function of time with  $T = 10.57$  and  $N = 100$ .

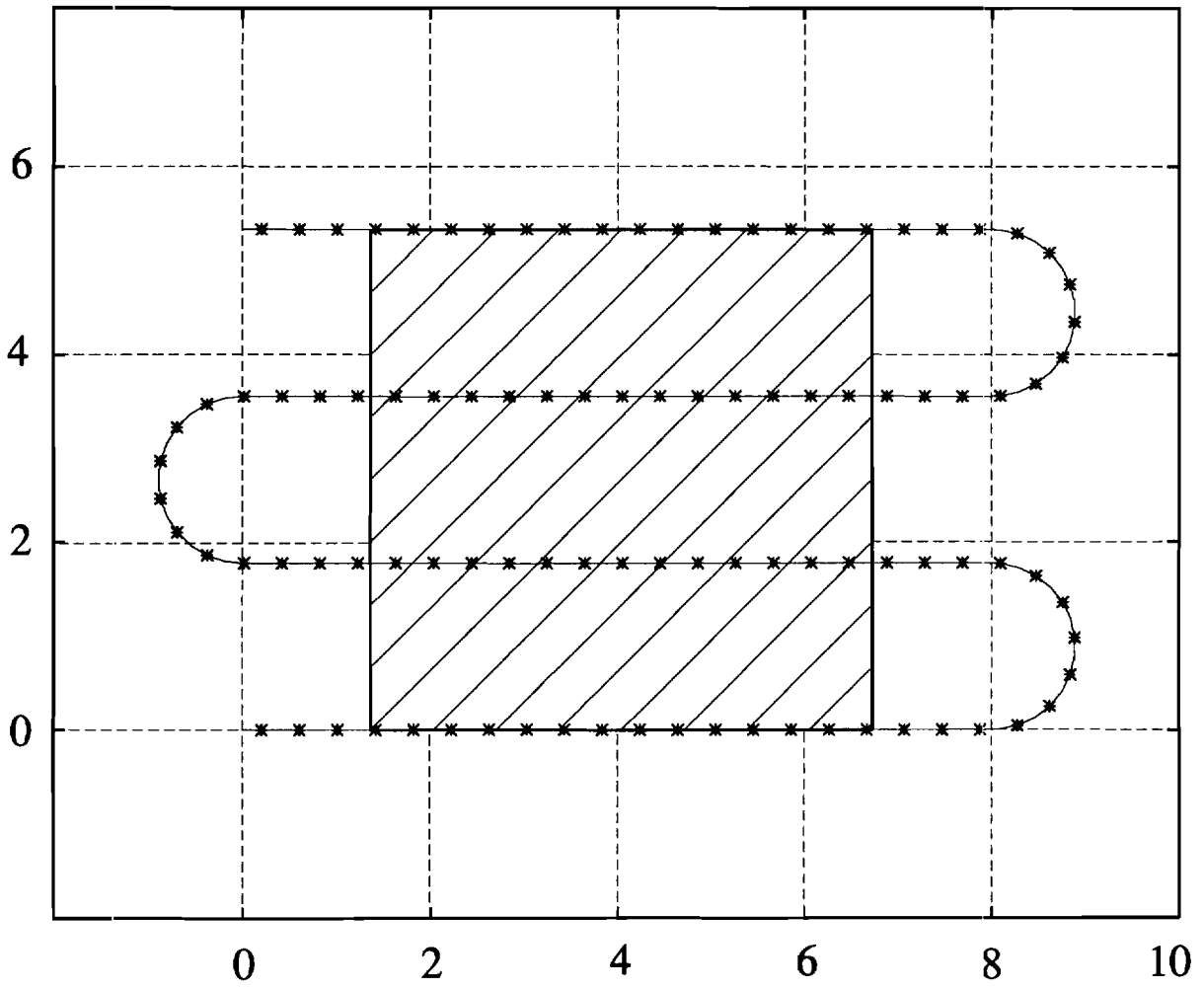


Fig. 2b. The XY coordinates of the trajectory  $\mathbf{p}_{\ell,d}(\tilde{\lambda}_{T,N}^{\text{lin}}(t))$  for the case  $\ell = 8$ ,  $d = 1\frac{7}{9}$ ,  $T = 10.57$  and  $N = 100$ . The panel is indicated by the shaded area.

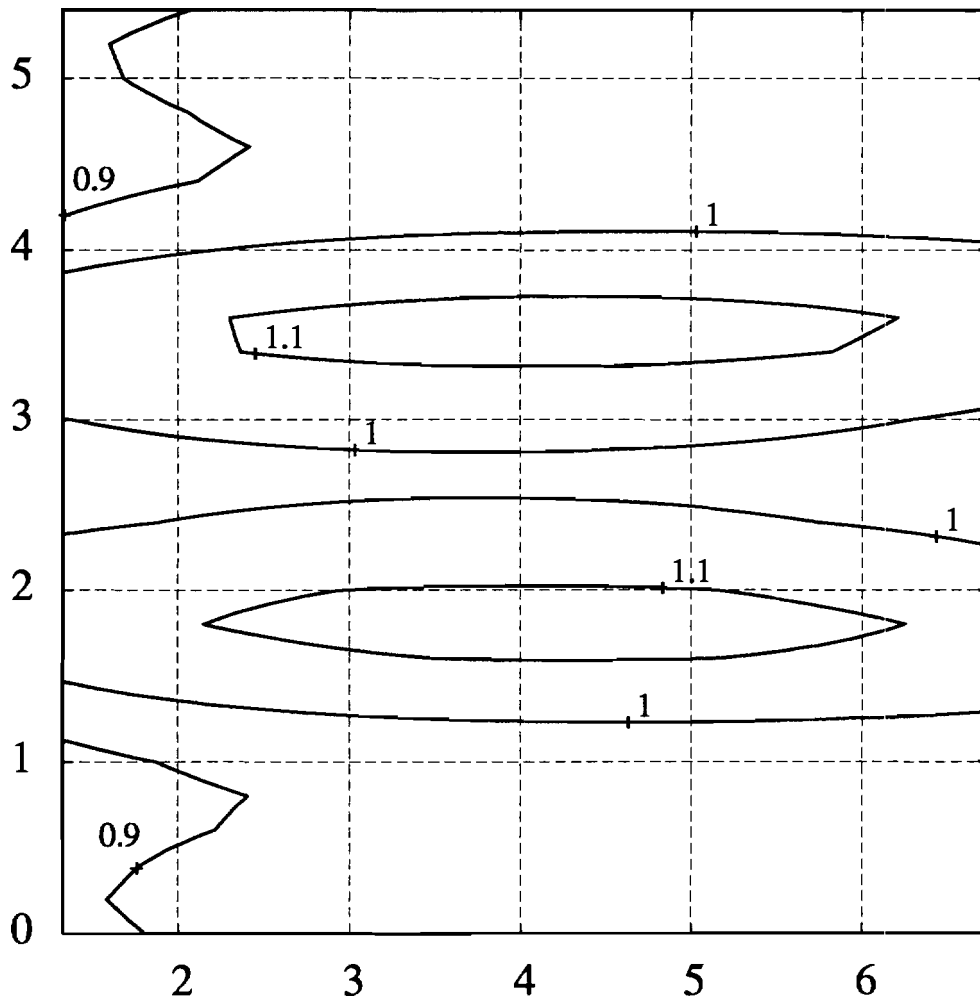
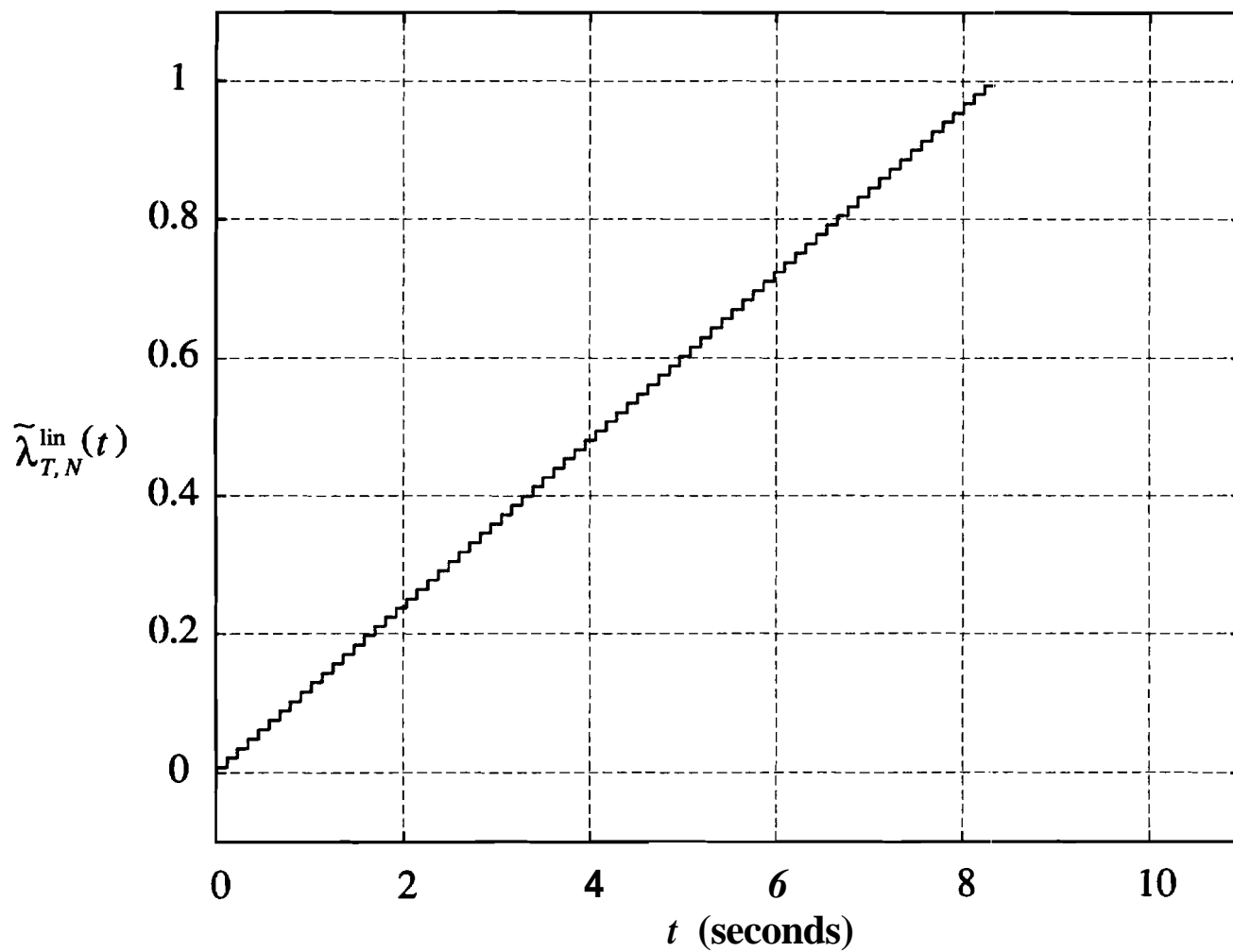


Fig. 2c. The contour plot for the panel's film thickness, which is a result of the trajectory of Fig. 2b.



**Fig. 3a.** A piecewise constant approximation to a linearly increasing function of time with  $T = 8.34$  and  $N = 74$ .

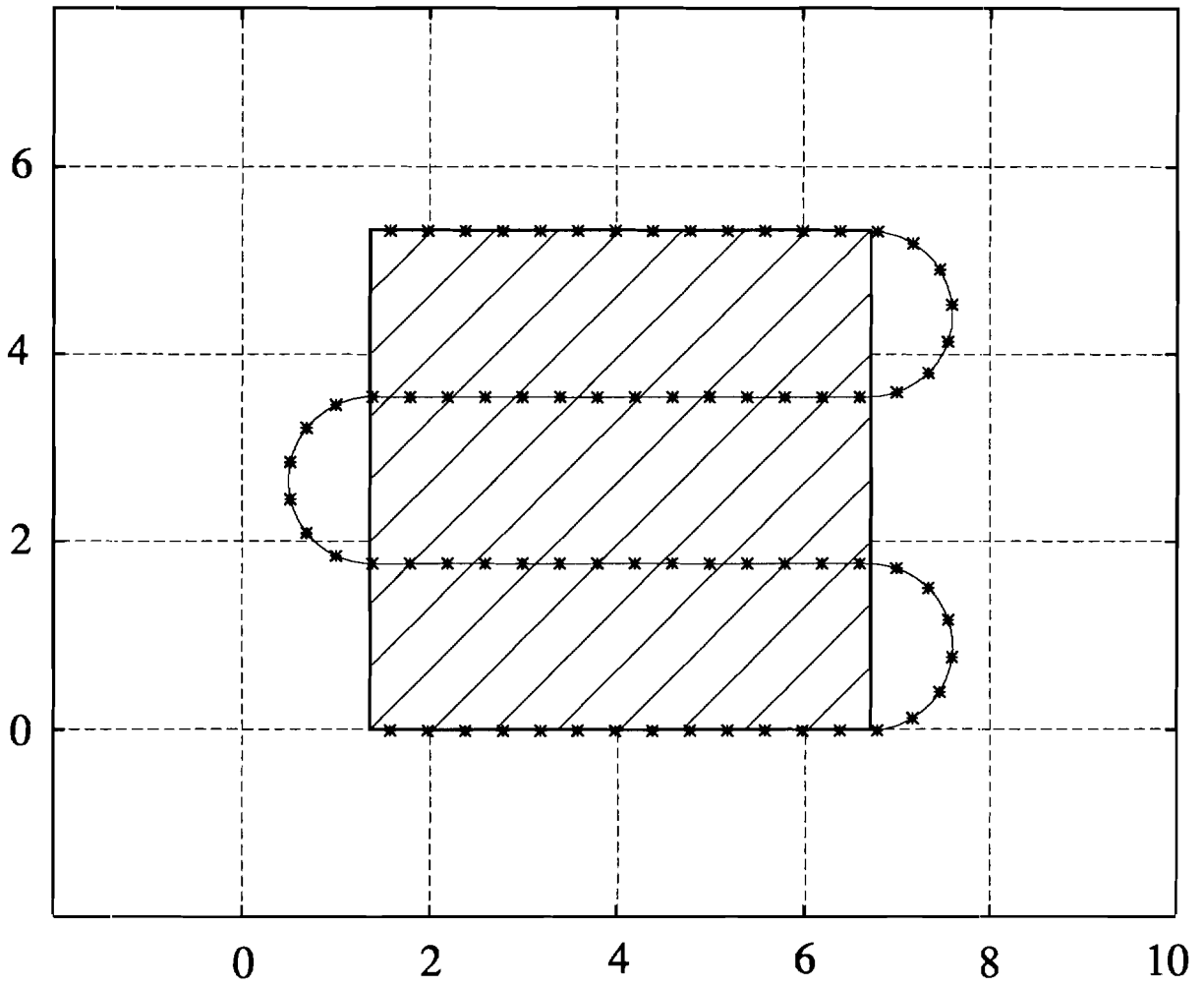


Fig. 3b. The XY coordinates of the trajectory  $\mathbf{p}_{\ell,d}(\tilde{\lambda}_{T,N}^{\text{lin}}(t))$  for the case  $\ell = 5$ ,  $d = 1\frac{7}{9}$ ,  $\mathbf{T} = 8.34$  and  $\mathbf{N} = 74$ . The panel is indicated by the shaded area.

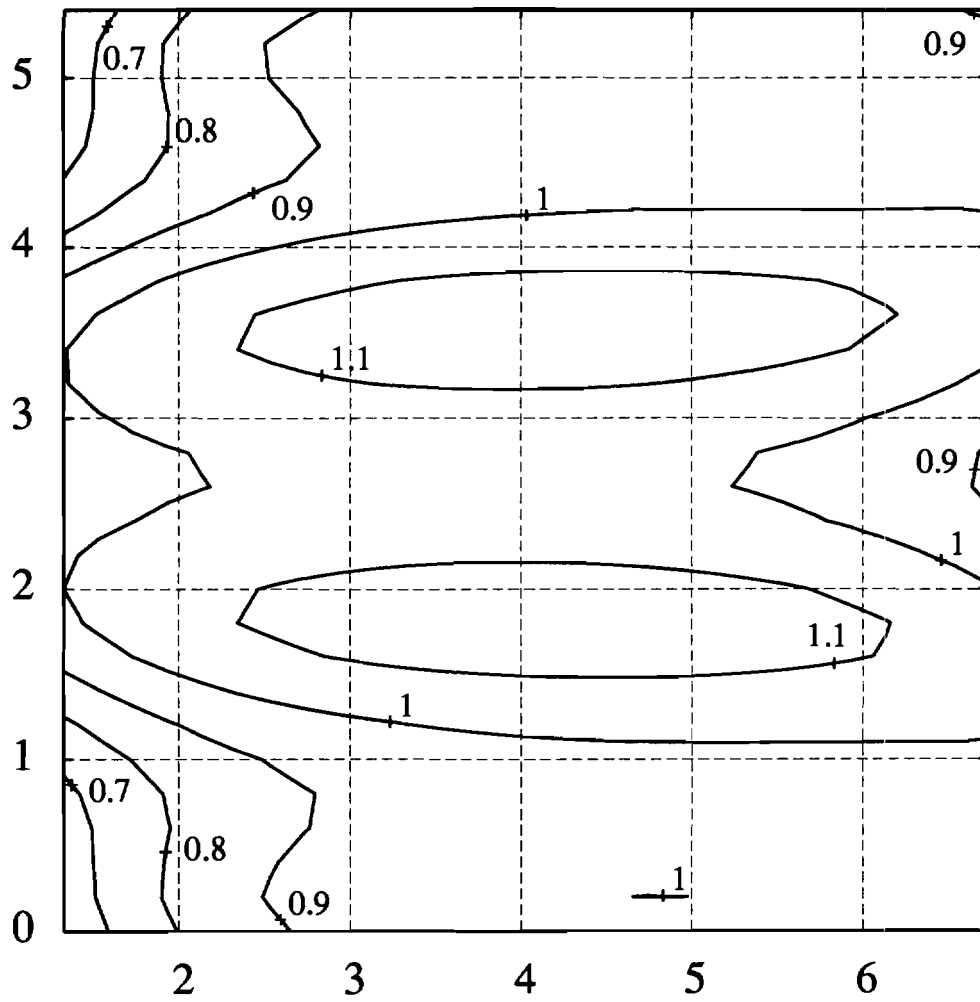


Fig. 3c. The contour plot for the panel's film thickness, which is a result of the trajectory of Fig. 3b.

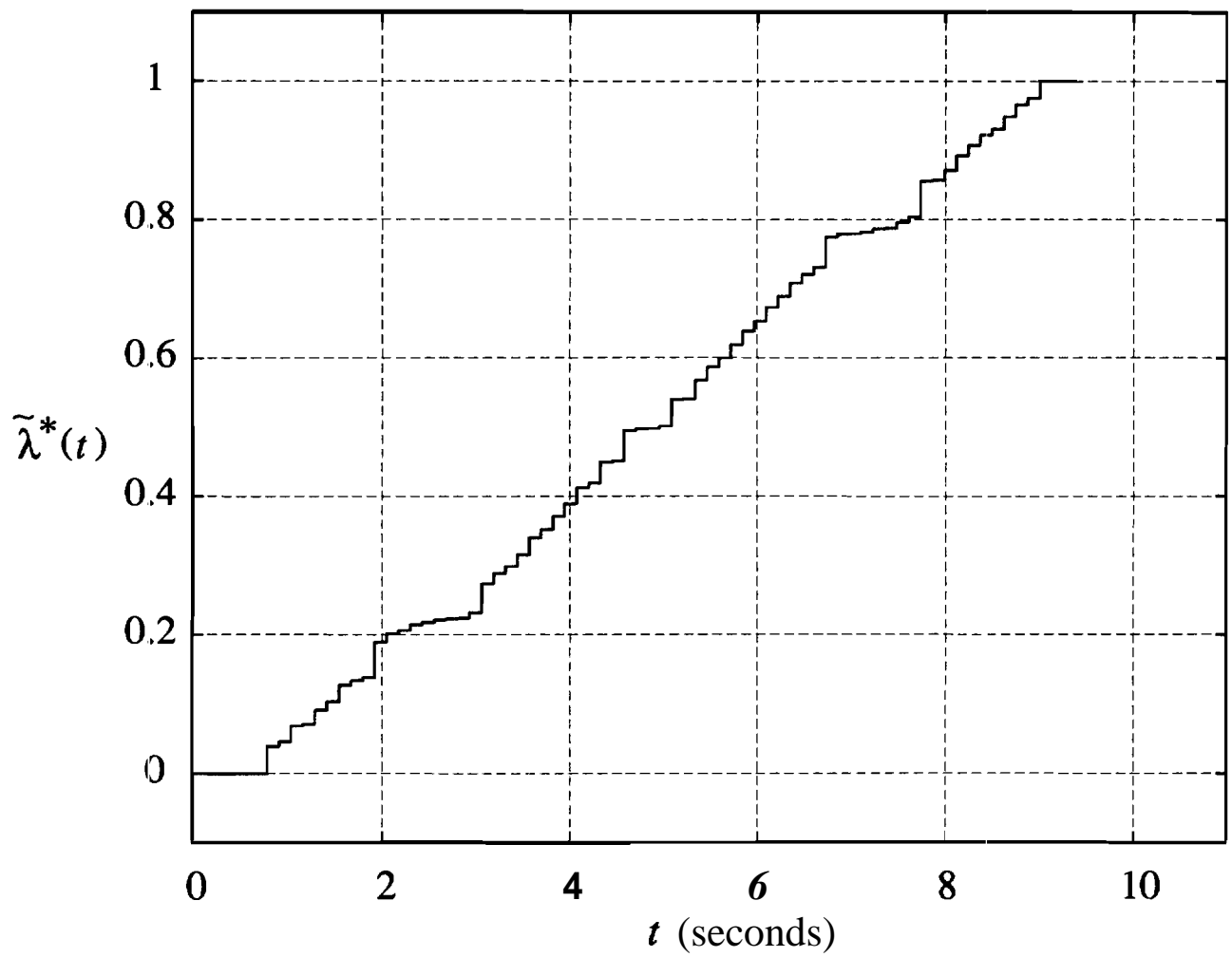


Fig. 4a. The optimal piecewise constant function of time with  $T = 9.37$  and  $N = 74$ .

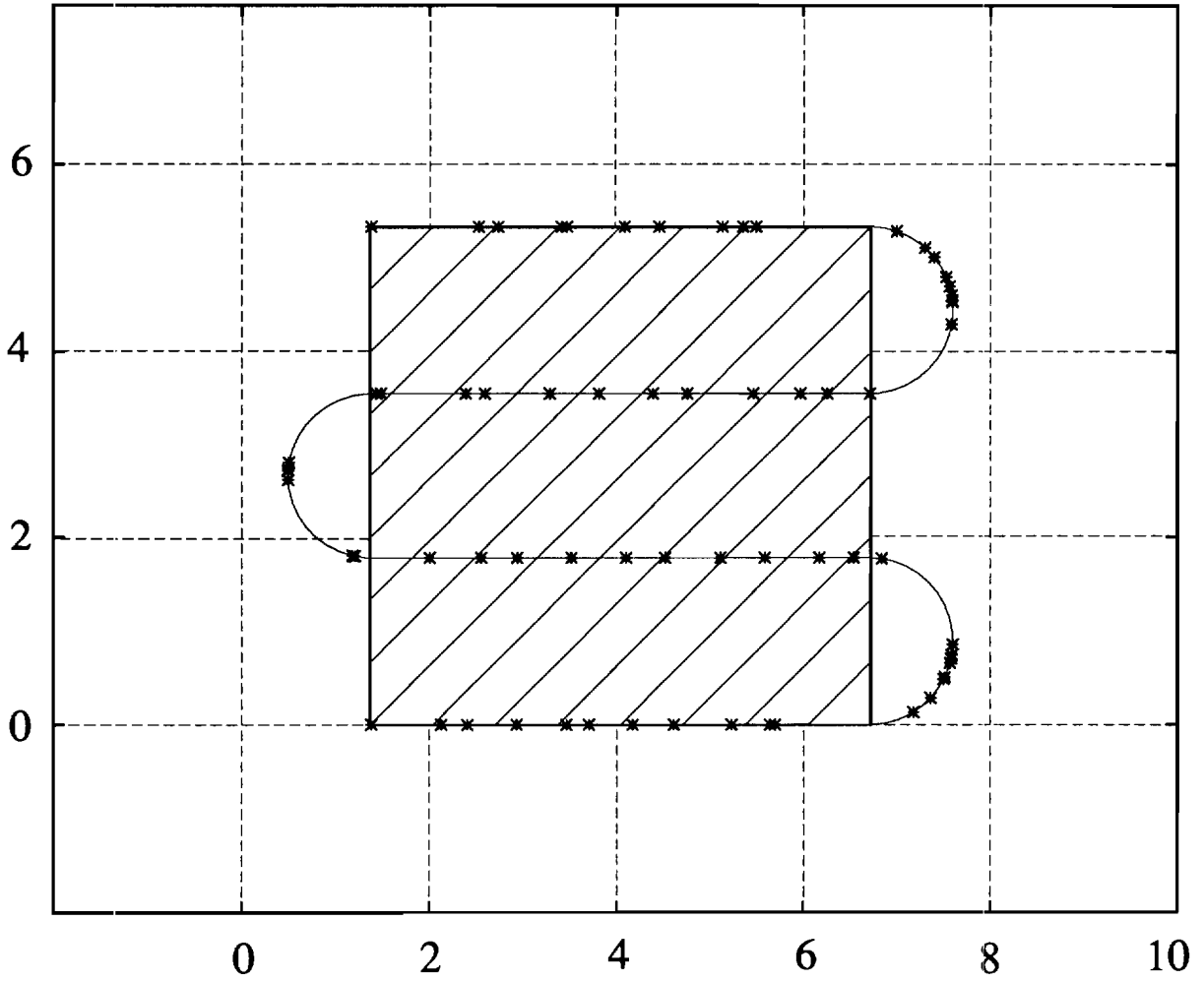


Fig. 4b. The  $XY$  coordinates of the trajectory  $p_{\ell,d}(\tilde{\lambda}_{T,N}^*(t))$  for the case  $\ell = 5$ ,  $d = 1\frac{7}{9}$ ,  $T = 9.37$  and  $N = 74$ . The panel is indicated by the shaded area.

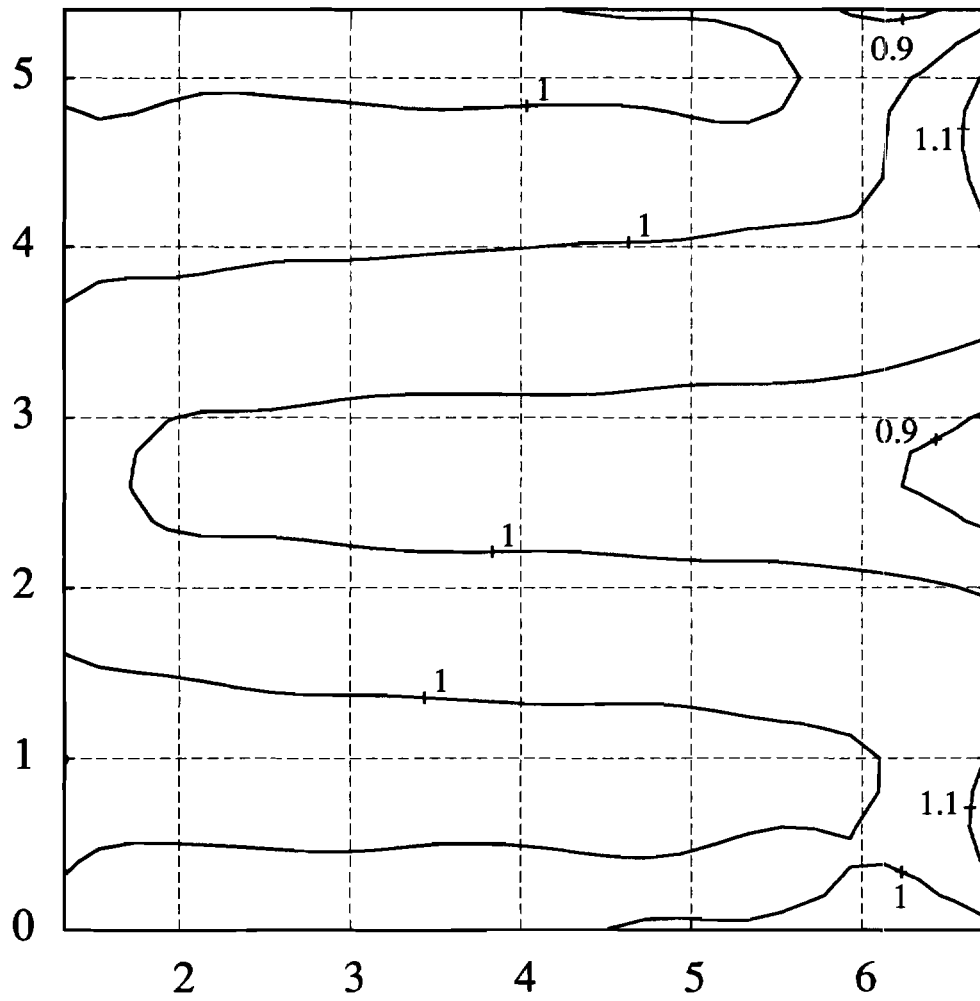


Fig. 4c. The contour plot for the panel's film thickness, which is a result of the trajectory of Fig. 4b.

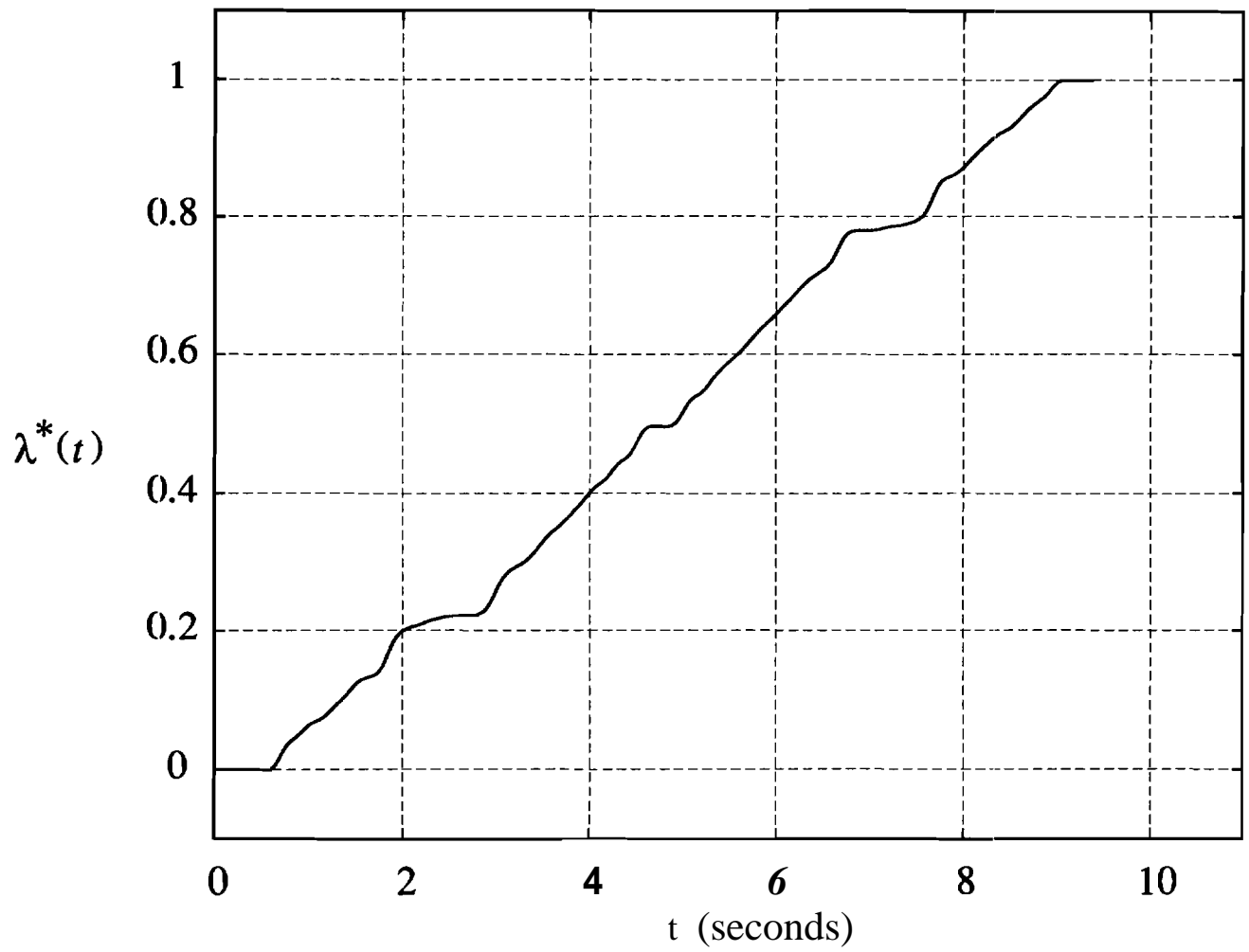


Fig. 5a. The optimal function of time with  $T = 9.37$  and  $N = 740$  (a cubic-spline interpolation of the function shown in Fig. 4a).

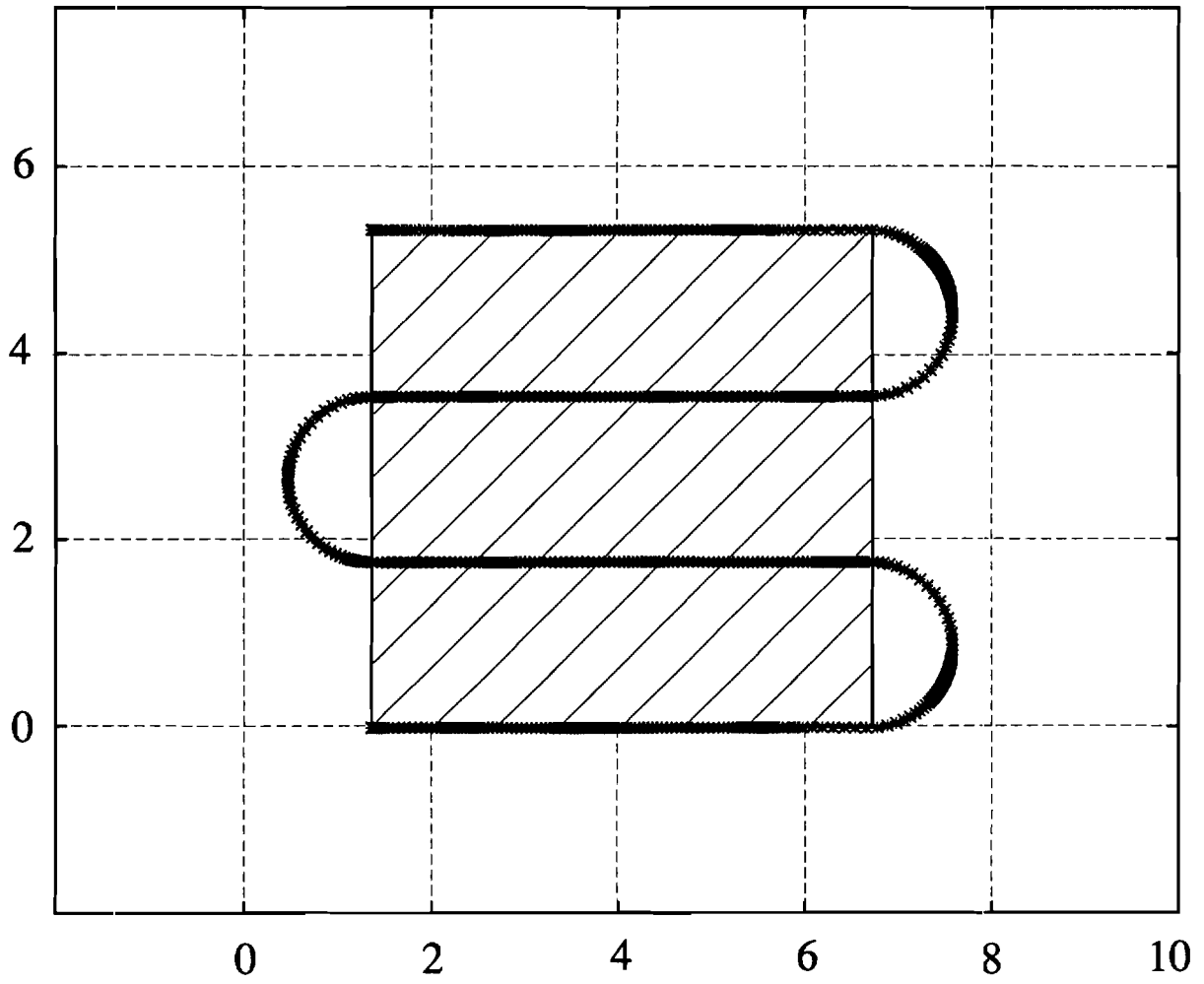
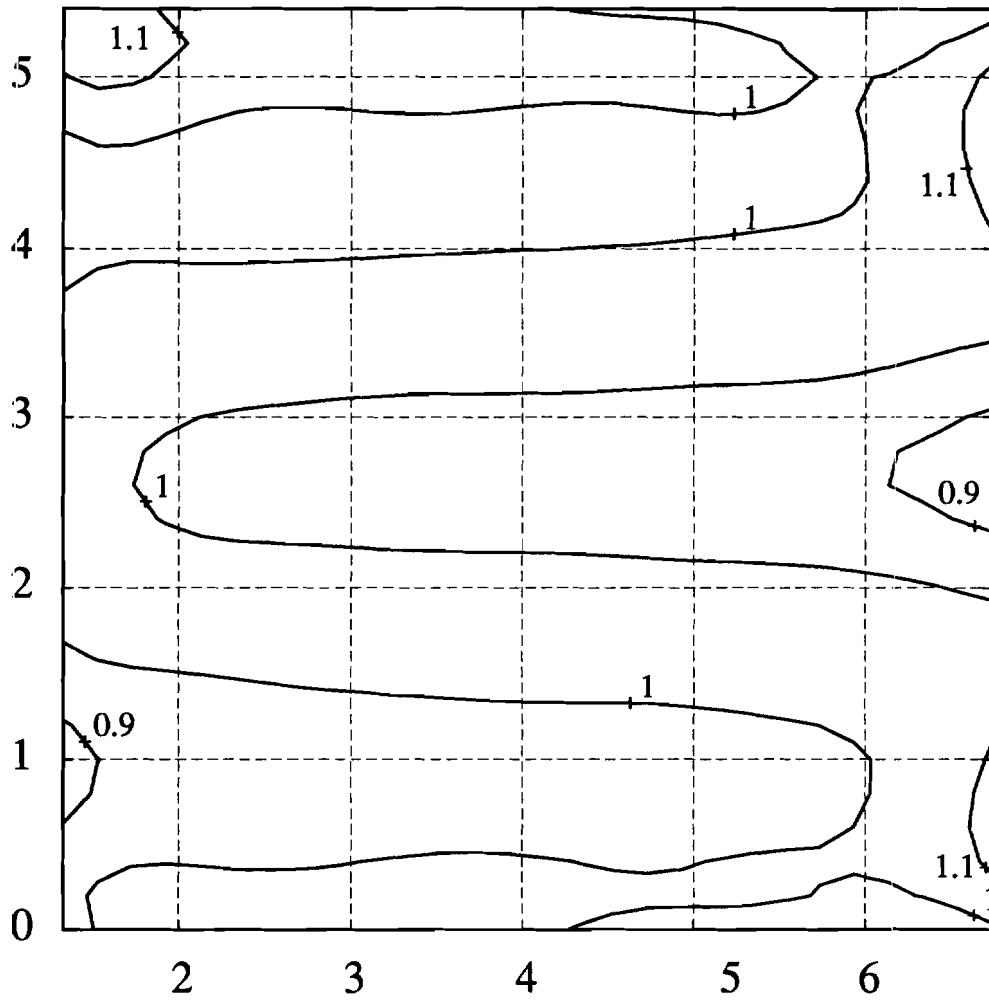


Fig. 5b. The XY coordinates of the trajectory  $\mathbf{p}_{\ell,d}(\lambda_{T,N}^{\text{lin}}(t))$  for the case  $\ell = 5$ ,  $d = 1\frac{7}{9}$ ,  $T = 9.37$  and  $N = 740$ . The panel is indicated by the shaded area.



**Fig. 5c.** The contour plot for the panel's film thickness, which is a result of the trajectory of **Fig. 5b**.